Investigation on the Drag Coefficient of the Steady and Unsteady Flow Conditions in Coarse Porous Media

Hadi Norouzi (hadinorouzi72@gmail.com)
University of Zanjan https://orcid.org/0000-0001-6082-3736
Jalal Bazargan
University of Zanjan
Faezah Azhang
University of Zanjan
Rana Nasiri
University of Zanjan

Research Article

Keywords: Drag Coefficient, Friction Coefficient, Hydraulic Gradient, Porous Media, Steady and Unsteady Flow

Posted Date: March 24th, 2021

DOI: https://doi.org/10.21203/rs.3.rs-332975/v1

Investigation on the Drag Coefficient of the Steady and Unsteady Flow Conditions in Coarse Porous Media

Hadi Norouzi [a*], Jalal Bazargan [b], Faezeh Azhang[c], Rana Nasiri[d]

a. PhD Candidate of Hydraulic Structures, Department of Civil Engineering, University of Zanjan, Zanjan, Iran (hadinorouzi72@gmail.com)

b. Associate Professor, Department of Civil Engineering, University of Zanjan, Zanjan, Iran (jbazargan@znu.ac.ir)

c. Masters of Hydraulic Structures, Department of Civil Engineering, University of Zanjan, Zanjan, Iran (faezehazhang73@yahoo.com)

d. Masters of Hydraulic Structures, Department of Civil Engineering, University of Zanjan, Zanjan, Iran (nasiri.rana@znu.ac.ir)

Abstract

The study of the steady and unsteady flow through porous media and the interactions between fluids and particles is of utmost importance. In the present study, binomial and trinomial equations to calculate the changes in hydraulic gradient (i) in terms of flow velocity (V) were studied in the steady and unsteady flow conditions, respectively. According to previous studies, the calculation of drag coefficient (C_d) and consequently, drag force (F_d) is a function of coefficient of friction (f). Using Darcy-Weisbach equations in pipes, the hydraulic gradient equations in terms of flow velocity in the steady and unsteady flow conditions, and the analytical equations proposed by Ahmed and Sunada in calculation of the coefficients a and b of the binomial equation and the friction coefficient (f) equation in terms of the Reynolds number (Re) in the porous media, equations were presented for calculation of the friction coefficient in terms of the Reynolds number in the steady and unsteady flow conditions in 1D

(one-dimensional) confined porous media. Comparison of experimental results with the results of the proposed equation in estimation of the drag coefficient in the present study confirmed the high accuracy and efficiency of the equations. The mean relative error (MRE) between the computational (using the proposed equations in the present study) and observational (direct use of experimental data) friction coefficient for small, medium and large grading in the steady flow conditions was equal to 1.913, 3.614 and 3.322%, respectively. In the unsteady flow condition, the corresponding values of 7.806, 14.106 and 10.506 % were obtained, respectively.

Keywords: Drag Coefficient, Friction Coefficient, Hydraulic Gradient, Porous Media, Steady and Unsteady Flow.

1 Introduction

Coarse-grained gravels (rockfill materials) have numerous applications in engineering including filtration, construction of gabions, lining of channels, stilling basins, ponds, and cobble stone dams as well as flood control.

In the fine-grained media, there is laminar flow with a linear relation between the hydraulic gradient and the flow velocity and flow follows Darcy's law (Eq. 1) (McWhorter et al. 1977). However, in the coarse-grained media, due to the presence of voids, the velocity of the flow is high with the flow tendency to turbulence (Hansen et al. 1995), with a nonlinear relation between the hydraulic gradient and flow velocity and low follows non-Darcy law. The equations for the calculation of hydraulic gradient in the non-Darcy media in the steady flow condition are classified into two groups of power and binomial equations, according to Eqs. 2 and 3 (Forchheimer, 1901; Leps, 1973; Stephenson, 1979).

$$i = \left(\frac{1}{k}\right)V \tag{1}$$

47 $$i = mV^n \quad (2)$$

48 $$i = aV + bV^2 \quad (3)$$

49 The binomial equation was proved by dimensional analysis by Ward (1964) and by the
50 Navier-Stokes equations by Ahmed and Sunada (1969) and has a higher accuracy and
51 efficiency in comparison to the exponential equation (Stephenson 1979, Leps 1973).

52 Ergun (1952) studied the coefficients of the binomial equation of the hydraulic gradient by
53 passing nitrogen gas through a cylinder with an area of 7.24 cm^2 that was filled with
54 aggregate and presented Eq. (4) to calculate the coefficients a, b.

55 $$a = 150\frac{\upsilon(1-n)^2}{d^2 g n^3} \quad , b = 1.75\frac{(1-n)}{g d n^3} \quad (4)$$

56 Ward (1964) presented Eq. (5), which can be proved using dimensional analysis, to calculate
57 the coefficients a and b in the free surface porous media.

58 $$a = \frac{\upsilon}{gk} \quad , b = \frac{C'_W}{g\sqrt{k}} \quad (5)$$

59 Kovacs (1980) studied a set of data with a Reynolds number range of 10 to 100 (according to
60 his definition of the Reynolds number) and presented an equation similar to that of Ergun
61 (Eq. (6)).

62 $$a = \frac{144\nu(1-n)^2}{g n^3 d^2} \quad , b = \frac{2.4(1-n)}{g n^3 d} \quad (6)$$

63 Ahmed and Sunada (1969) presented Eq. (7) to calculate the coefficients a and b using the
64 Navier-Stokes equations.

65 $$a = \frac{\mu}{\rho g k} \quad , b = \frac{1}{g\sqrt{ck}} \quad ,(7) \qquad K = Cd^2$$

Ergun-Reichelt presented an equation for calculation of the coefficients a, b (Eq. (8)) (Fand and Thinakaran, 1990).

$$a = 214\frac{M^2(1-n)^2\nu}{gn^3d^2} \quad , b = 1.57\frac{M(1-n)}{gn^3d} \quad , M = 1+\frac{2}{3}\frac{d}{D(1-n)} \tag{8}$$

Equations (4) to (8) and several equations including those proposed by (Muskrat 1937; Engelund 1953; Irmay 1958; Stephenson 1979; Jent 1991; Kadlec and Knight 1996; Sidiropoulou et al. 2007; Sedghi and Rahimi 2011) were presented to calculate the coefficients of the binomial equation (a, b) in steady flow conditions. A semi-analytical solution of the nonlinear differential equations constructing a fully saturated porous medium is presented by (Abbas et al. 2021).

A comprehensive equation with respect to the effects of unsteady flow conditions was proposed by Polubarinova-Kochino (1952) (Eq. (9)) (Hannoura and McCorcoudale, 1985).

$$i = aV + bV^2 + c\left(\frac{dV}{dt}\right) \tag{9}$$

Where the coefficient of the third term (c) is obtained using Eq. (10).

$$c = \frac{n + C_m(1-n)}{ng} \tag{10}$$

Where C_m represents the proportion of fluid that vibrates with the vibration of the particle. In other words, C_m is the added mass coefficient.

Hannoura and McCorquodale (1985) performed an experimental study and indicated that C_m was insignificant and negligible. In other words, by removing C_m from Eq. (10), the third term of Eq. (9) can be expressed as Eq. (11).

$$c\left(\frac{dV}{dt}\right) = \frac{1}{g}\left(\frac{dV}{dt}\right) \tag{11}$$

where V is flow velocity (m/s), k is hydraulic conductivity (s/m), i is hydraulic gradient, m and n are values dependent on the properties of the porous media, fluid and flow, while a and b are coefficients that are dependent on the properties of the porous media as well as the fluid.

Shokri et al. (2011) experimentally studied unsteady flow in a free surface coarse-grained porous media and concluded that the third term ($c\left(\frac{dV}{dt}\right)$) has insignificant effect on the accuracy of calculations.

In the present study, the binomial (Eq. 3) and trinomial (Eq. 8) equations were used to calculate the changes in hydraulic gradient in terms of velocity in steady and unsteady flow conditions, respectively.

The simulated annealing algorithm is often used for water resources management, model calibration, decision making, etc. (Bechler et al. 2013; Cao and Ye 2013; Jiang et al. 2018). (Hu et al. 2019) Kriging-approximation simulated annealing (KASA) optimization algorithm has been used to optimize the flow parameters in the porous media.

Particle swarm optimization (PSO) algorithm is a population-based evolutionary algorithm and is used in civil engineering and water resources optimization problems such as reservoir performance (Nagesh Kumar and Janga Reddy, 2007), water quality management (Afshar et al. 2011, Lu et al. 2002, Chau, 2005) and optimization of the Muskingum method coefficients (Chu and Chang 2009, Moghaddam et al. 2016, Bazargan and Norouzi 2018, Norouzi and Bazargan 2020, Norouzi and Bazargan 2021). Therefore, in the present study, the particle swarm optimization (PSO) algorithm was used to optimize the coefficients of the Forchheimer binomial equation (Eq. 3) as well as the Polubarinova-Kochino trinomial equation (Eq. 8).

In addition to the above classification, flow in the coarse-grained media can be classified into the following two general groups.

A: Free surface flow through and on coarse-grained layers such as gabions and gravel dams in which the flow is in contact with the free environment on one side.

B: Confined flow through coarse-grained layers such as coarse-grained filters of rockfill dams and coarse-grained layers confined between concrete elements and fine materials of hydraulic structures. In such layers, flow from all sides is in contact with an impermeable layer or a layer with low permeability in comparison to gravel materials.

The study of flow through confined porous media is of great importance in geology (Lei et al. 2017), petroleum (Song et al. 2014) and industry (Rahimi et al. 2017). Flow through pressurized porous media has been studied experimentally and numerically by (Ingham and Pop 2005; Sheikh and Pak 2015; and Zhu et al. 2016). The study of fluid flow in porous media is performed by a network of capillary pipes with a microscopic approach by (Hoang et al. 2013). (Hsu and Chen 2010) proposes a multiscale flow and transport model in three-dimensional fractal random fields for use in porous media.

Estimation of drag force due to flow-aggregate interactions is very important in modeling of confined porous media (Sheikh and Qiu, 2018). Pore-scale drag and relative motion between fluid and aggregates are important due to the formation of non-uniform velocity and consequently, the formation of non-uniform force (Sheikh and Qiu, 2018). (Ergun 1952; Wen and Yu 1966; Di Felice 1994; Schlichting and Gersten 2000; Hill et al. 2001a; Hill et al. 2001b; Van der Hoef et al. 2005; Bird et al. 2007; Yin and Sundaresan 2009; Zhang et al. 2011; Rong et al. 2013) studied the drag force in the confined porous media considering a certain number of particles. The flow regime and drag force of a single particle are different from those of interactive particles (Zhu et al. 1994; Liang et al. 1996; Chen and Wu 2000).

The accuracy and efficiency of the presented empirical equations for calculation of the drag force have not been evaluated and compared for a wide range of porosity and Reynolds numbers. In other words, the relation between drag force and Reynolds number has been studied experimentally or numerically in previous studies. Accurate calculation of drag coefficient and drag force and its application in one-dimensional analysis of steady flow in porous media (gradually varied flows) has increased the accuracy of calculations, especially in sections with high curvature of the longitudinal profile of water surface (Gudarzi et al. 2020). To predict the flow characteristics in porous media, it is very important to acquire the structures of the porous media. However, it is difficult to measure the three-dimensional microstructures of high-resolution porous media due to the expensive cost of the equipment (Zhang et al. 2016).

Since the drag force (F_d) is a function of the drag coefficient (C_d) and C_d is a function of the friction coefficient (f), using binomial and trinomial equations, Darcy-Wiesbach equation, Ahmed and Sunada analytical equation to calculate coefficients a, b and changes of coefficient f in terms of the Reynolds number (Re) in porous media, equations were presented in the present study to calculate f in terms of Re in steady and unsteady flow conditions in 1D confined porous media. Comparison of the results of the proposed equations with experimental data indicated the high accuracy and efficiency of the proposed equations. In other words, in the present study, equations were presented for steady and unsteady flow conditions in porous media and applicable for any number of particles as well as all Reynolds numbers.

2 Materials and methods

2.1 Experimental data

156 The experiments were performed in the Laboratory of the Faculty of Civil Engineering of
157 Zanjan University, Zanjan, Iran on a steel cylinder with a diameter of 16 cm and a length of
158 70 cm, of which 40 cm was filled with aggregates considering steady and unsteady flow
159 conditions. In order to develop unsteady flow condition using the gravity method, a tank was
160 installed at a height of 13 meters above the cylinder inlet on the roof of the faculty. To
161 discharge the cylinder outflow, a tank was installed in the laboratory. Using a camcorder,
162 water height in the discharge tank was recorded at different times and then, using the
163 volumetric method, discharge of the unsteady flow was recorded at different times. To
164 measure water depth, piezometers were installed at the beginning and end of the cylinder.
165 The tanks used, aggregates in three gradations (small, medium and large) and the steel
166 cylinder are shown in Figure 1. The characteristics of the aggregates and gradation curves of
167 the three gradations (small, medium and large) are shown in Table 1 and Fig. 2, respectively.
168 Figure 3 and Figure 4 show changes in hydraulic gradient (i) versus flow velocity (V) for all
169 three types of small, medium and large grained materials in the steady and unsteady flow
170 conditions, respectively.

171

172 **a**

b

c

Figure 1. Schematic view of the experimental setup, a) the installed tank on the roof, b) the tank and cylinder installed in the laboratory, and c) steel cylinder

Table 1. Characteristics of the experimental materials

Materials	d_0 (mm)	d_{10} (mm)	d_{30} (mm)	d_{50} (mm)	d_{60} (mm)	d_{100} (mm)	C_u	C_c	porosity
Small	4	7	10	12.5	14.5	22	1.69	0.69	0358
Medium	4.75	14.5	18.5	19	21.3	32	1.16	0.95	0.410
Large	12.7	22.7	23.9	22	25.05	32	1.11	0.99	0.448

In Table 1, the coefficient of uniformity (C_u) and the coefficient of curvature (C_c) were equal to $\frac{D_{60}}{D_{10}}$ and $\frac{(D_{30})^2}{D_{10} * D_{60}}$, respectively.

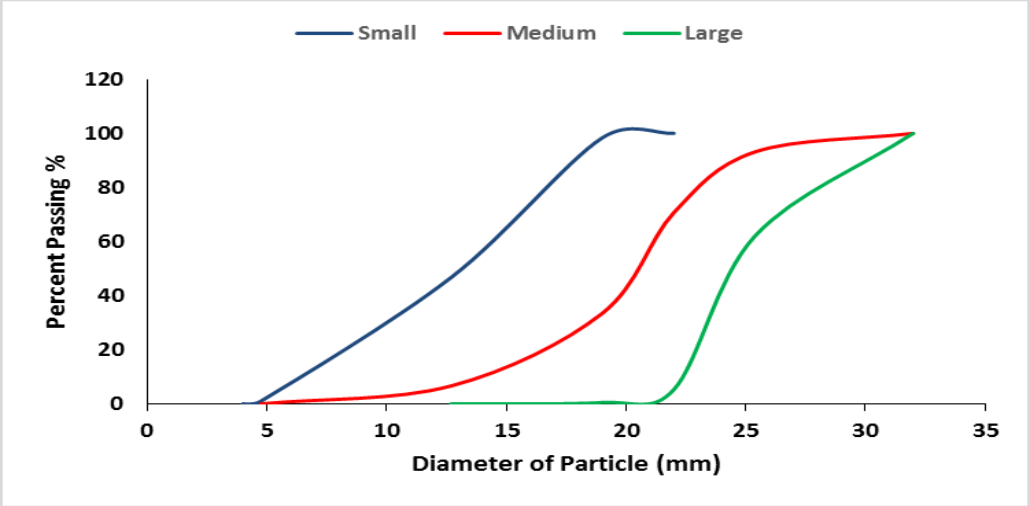

Figure 2. Gradation curve of different materials

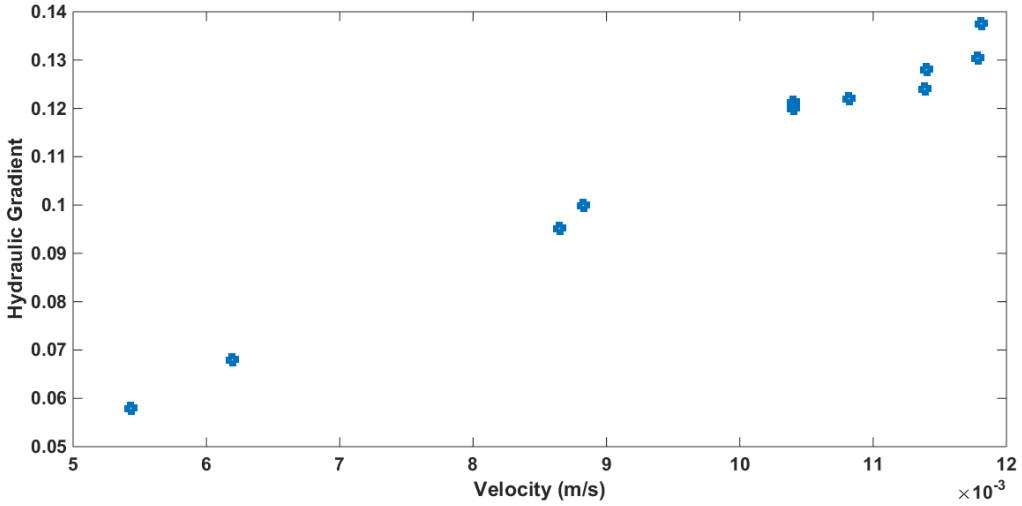

193

194 **a.** Small

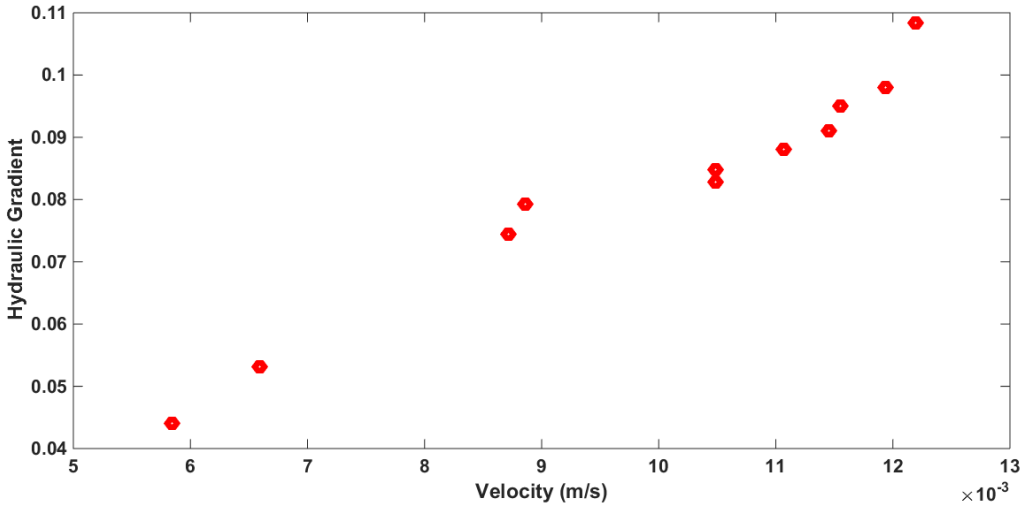

195

196 **b.** Medium

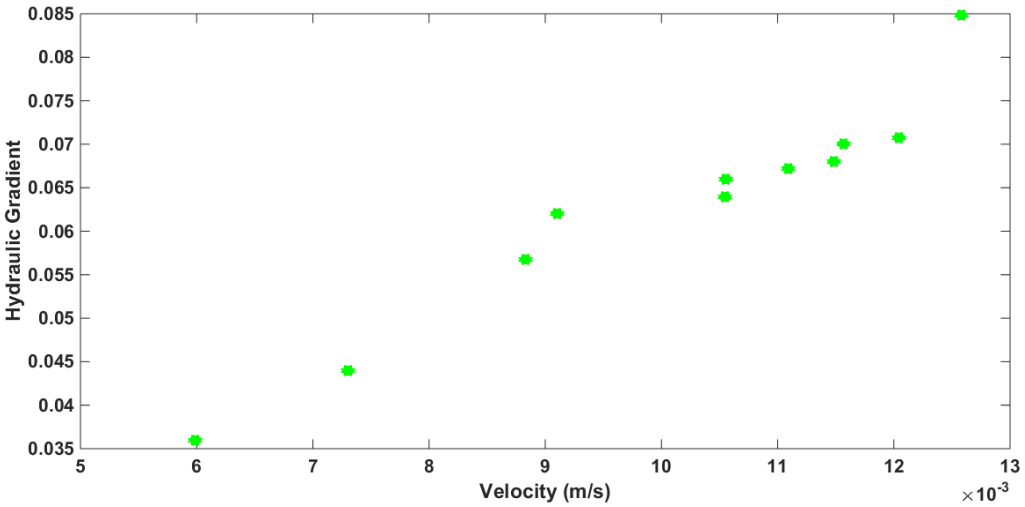

197

198 **c.** Large

199 **Figure 3.** Changes in hydraulic gradient versus steady flow velocity recorded in the
200 laboratory

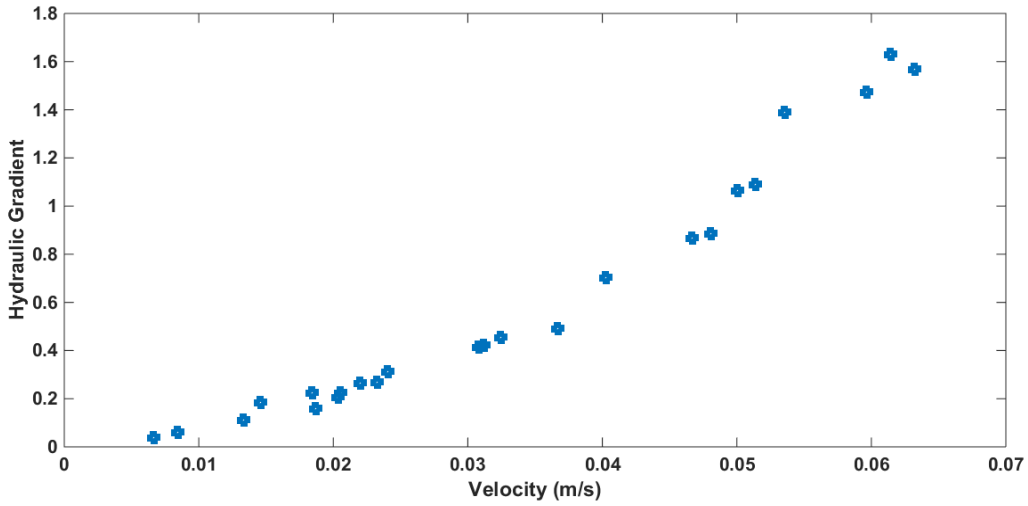

201

202 **a.** Small

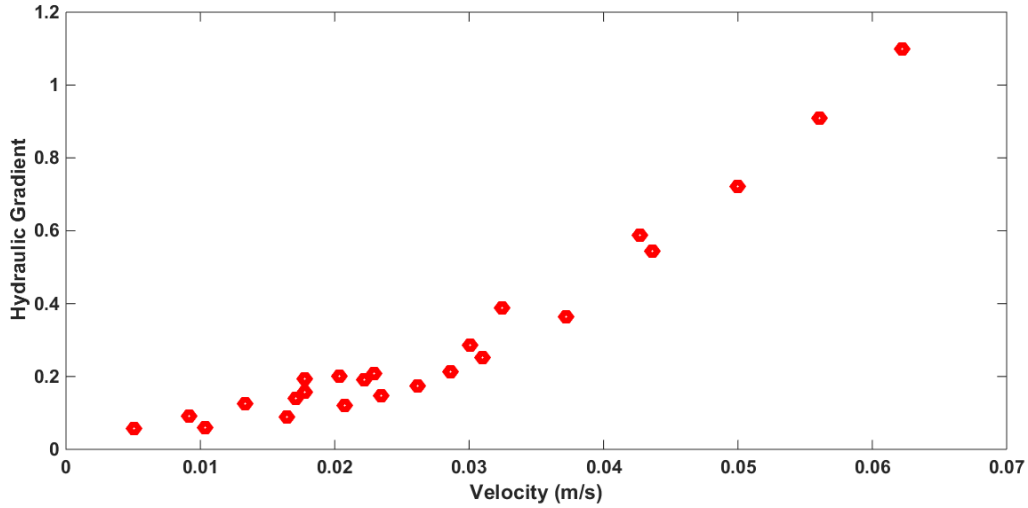

203

204 **b.** Medium

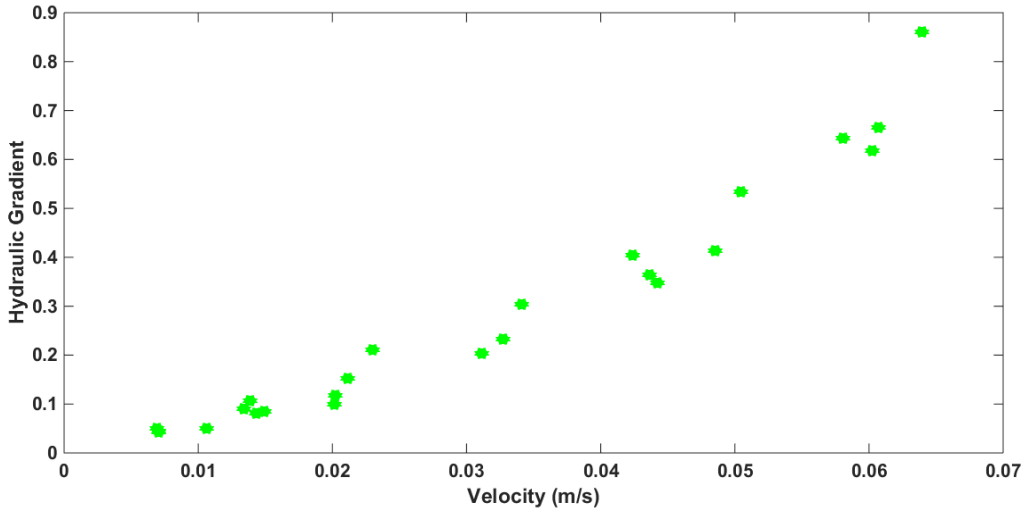

205

206 **c.** Large

207 **Figure 4.** Changes in hydraulic gradient versus unsteady flow velocity recorded in the
208 laboratory

2.2 Particle Swarm Optimization (PSO) Algorithm

PSO method is also a population based evolutionary search optimization method inspired from the movement of bird flock (swarm) (Eberhart and Kennedy 1995; Chau 2007; Clerc and Kennedy 2002). The basic idea in PSO is based on the assumption that potential solutions are flown through hyperspace with acceleration towards more optimum solutions. Each particle adjusts its flying according to the experiences of both itself and its companions. During the process; the overall best value attained by all the particles within the group and the coordinates of each element in hyperspace associated with its previous best fitness solution are recorded in the memory (Chau 2007; Kumar and Reddy 2007). The details of PSO can be obtained elsewhere (Shi and Eberhart 1998; Clerc and Kennedy 2002; Chau 2007; Gurarslan and Karahan 2011; Karahan 2012; Di Cesare et al. 2015). Various algorithms have been used to optimize the parameters of the Forchheimer equation and other methods and other issues that need to be optimized, one of the fastest, most acceptable and most widely used is the PSO algorithm, which has been confirmed by previous researchers.

since in previous studies, efficiency, high convergence speed and proper accuracy of the PSO algorithm have been examined and approved, therefore, among different algorithms, the PSO algorithm is selected to optimize the Forchheimer equation coefficients (a, b) and Polubarinova-Kochino equation coefficient (a, b, c).

To evaluate the optimum values of the binomial equation coefficients (a, b) and the trinomial equation coefficients (a, b, c), the minimization of the Mean Relative Error (MRE), which is defined using Eq. (12), was used as the objective function in the Particle Swarm Optimization algorithm.

$$MRE = \frac{1}{n}\sum_{i=1}^{n}\left|\frac{i_i - I_i}{i_i}\right| * 100 \tag{12}$$

232 Where i_i and I_i are observed and calculated values of hydraulic gradient using binomial and
233 trinomial equations, respectively. The flowchart used in the present study is presented in
234 Figure 5.

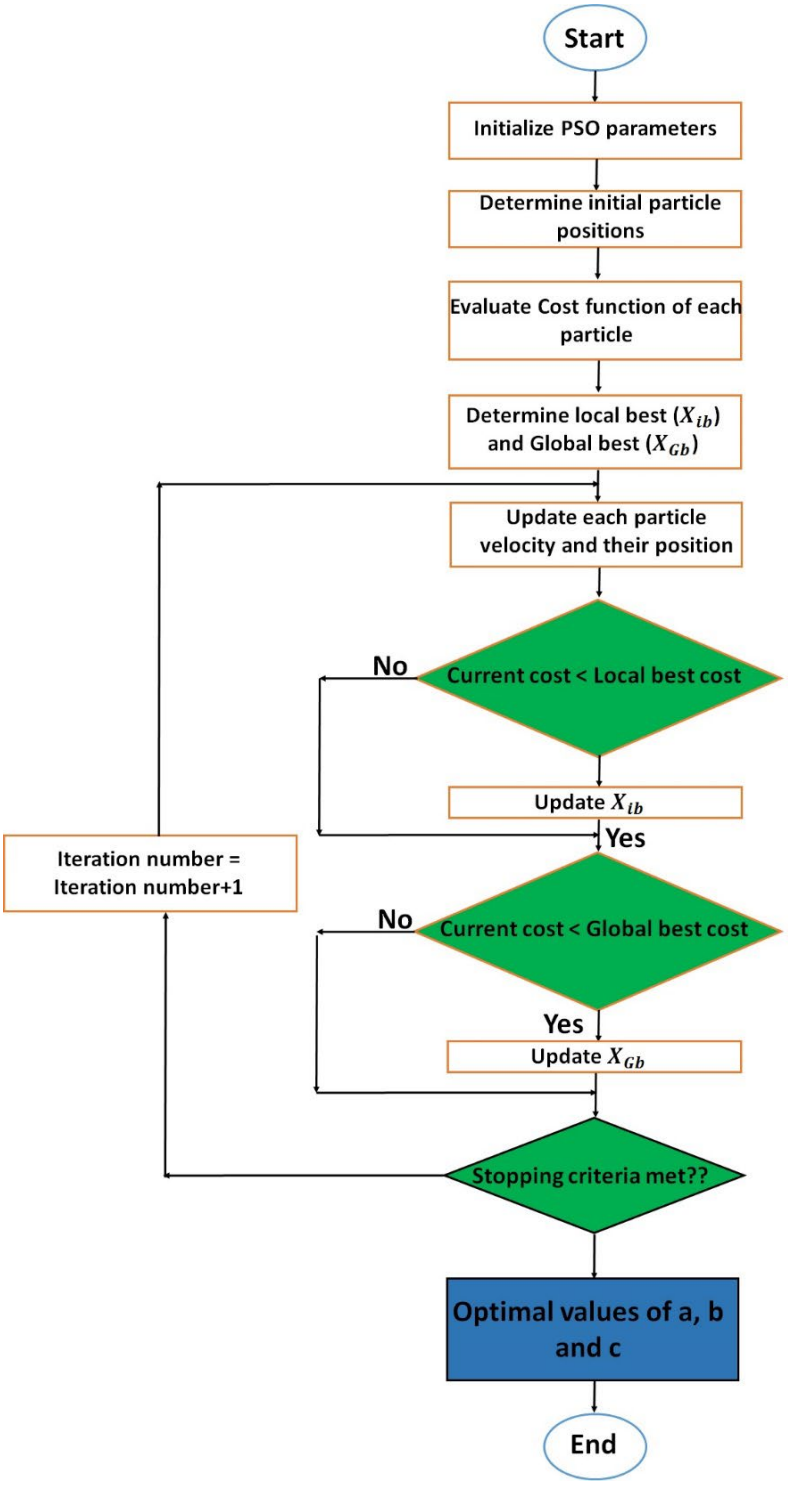

235

236 **Figure 5.** Particle Swarm Optimization (PSO) algorithm

3 Results and Discussion

3.1 Binomial (steady flow condition) and trinomial (unsteady flow condition) equations

The hydraulic gradient in a coarse grained media is equal to the slope of the energy line (S_f) (Stephenson 1969; Bari and Hansen 2002; Bazargan and Shoaei 2006). The calculation of hydraulic gradient is of great importance in the steady flow (using the gradual variable flow theory that analyzes flow one-dimensionally as well as the solution of the Parkin equation that analyzes flow two-dimensionally) and unsteady flow (solving Saint-Venant equations) analysis.

The binomial equation for the steady flow through porous media has been presented by Forchheimer and equations for calculation of coefficients a and b were also presented using dimensional analysis (Ward 1964) and Navier-Stokes equations (Ahmed and Sunada 1969). In the present study, the PSO algorithm was used to optimize the coefficients of the binomial equation (a, b). The values of the mentioned coefficients as well as the mean relative error (MRE) between the computational and observational hydraulic gradients for all three types of gradation (small, medium and large) are shown in Table 2.

Table 2. Optimized values of coefficients a and b and mean relative error (MRE) of hydraulic gradient in steady flow condition

Materials	a (s/m)	b (s^2/m^2)	MRE %
Small	10.584	64.043	1.913
Medium	7.981	13.705	3.614
Large	5.965	8.635	3.322

(Shokri et al. 2012; Hannoura and McCorquodale 1985) indicated that the third term of the trinomial equation (Eq. 9) is negligible in calculation of the hydraulic gradient in the free surface porous media. Hosseini and Joy (2007) used the coefficients of the binomial equation

in steady flow condition to study the hydraulic gradient and solve the Saint-Venant equations in the unsteady flow condition in porous media. The experimental results of the present study, which were obtained using a confined porous media (steel cylinder), indicated the high accuracy of the trinomial equation in comparison to the binomial equation in estimation of the hydraulic gradient changes in terms of unsteady flow velocity. Table 3 shows the values of the coefficients a and b of the binomial equation and the coefficients a, b, c of the trinomial equation when the values of the hydraulic gradient relative to the unsteady flow velocity are used to optimize the coefficients. In addition, the values of the mean relative error (MRE) between the computational and observational hydraulic gradients in the unsteady flow condition using the coefficients a and b obtained from the steady flow condition (as recommended by Hosseini and Joy 2007), coefficients a and b obtained from the unsteady flow condition by assuming an insignificant value of coefficient c in the trinomial equation (as recommended by Hannoura and McCorquodale 1985; Shokri et al. 2012) and by using coefficients a, b, c and trinomial equation are shown in Table 3. It is worth noting that the mentioned coefficients were optimized using the PSO algorithm.

Table 3. Values of the optimized coefficients a and b using steady and unsteady flow data and coefficients a, b, c of unsteady flow data and mean relative error (MRE) values of hydraulic gradient of unsteady flow

Regime	Equations	Coefficients	Small	Medium	Large
Steady	**Binomial**	a (s/m)	10.584	7.91	5.965
		b (s^2/m^2)	64.043	13.705	8.635
		MRE %	25.567	25.923	21.306
Unsteady	**Binomial**	a (s/m)	3.848	5.255	5.411
		b (s^2/m^2)	331.714	165.084	80.344
		MRE %	10.024	22.599	12.941
Unsteady	**Trinomial**	a (s/m)	2.859	2.225	3.704
		b (s^2/m^2)	352.622	165.336	107.186
		c (s^2/m)	10.369	51.369	14.581
		MRE %	7.806	14.106	10.506

As can be seen from Table 3, if the coefficients a and b obtained from the steady flow condition were used to calculate the changes in the hydraulic gradient relative to the unsteady flow velocity, the mean relative error (MRE) values of 25.567, 25.923, and 21.306 were obtained for the small, medium and large grained materials, respectively. In the case of using the coefficients a and b obtained from the unsteady flow data, the corresponding MRE values of 10.024, 22.599 and 12.941%, were obtained, respectively. In addition, by using the optimized coefficients a, b, and c of the trinomial equation, the corresponding MRE values of 7.806, 14.106 and 10.506% were obtained, respectively. The MRE values of the trinomial equation in comparison to those of the binomial equation in case of using the coefficients a and b obtained from the unsteady flow condition for three gradation types improved by 22, 38 and 19%, respectively. The corresponding values in case of using the coefficients a and b obtained from the steady flow condition improved by 70, 46 and 51%, respectively. In other words, in order to calculate the hydraulic gradient in the unsteady flow condition, the use of the coefficients a, b, and c of the unsteady flow and the trinomial equation, coefficients a and

298 b obtained from the unsteady flow data, and coefficients a and b obtained from the steady
299 flow data were more accurate, respectively.

300 **3.2 Drag coefficient in porous media**

301 In addition to power equations (Eq. 2) and Forchheimer binomial equation (Eq. 3), one of the
302 methods of flow analysis in porous media is the use of friction coefficient (f) in terms of
303 Reynolds number (Re). Accordingly, the flow energy loss in porous media is obtained using
304 an equation similar to the Darcy-Weisbach equation (Stephenson 1979; Herrera and Felton
305 1991). For the confined flow in the pipes, the Darcy-Wiesbach equation is expressed using
306 Eq. (13).

307 $$h_f = f\frac{L}{d}.\frac{V^2}{2g} \tag{13}$$

308 Where f is the (dimensionless) friction coefficient, L is the pipe length (m), d is the pipe
309 diameter (m), V is flow velocity (m/s), g is the acceleration of gravity (m/s^2), and h_f is the
310 energy loss (m).

311 Since h_f/L is equal to the hydraulic gradient, Eq. (13) can be rewritten as Eq. (14).

312 $$i = \frac{f}{d}.\frac{V^2}{2g} \tag{14}$$

313 Leps (1973) indicated the velocity corresponding head in the above equations as $\frac{V^2}{mg}$, with m
314 value of 2 according to the Darcy-Wiesbach equation in pipes. Stephenson (1979) assumed
315 the formation of the porous media inside a set of winding tubes within a set of aggregates
316 with pores, considered the value of m in the energy loss (h_f) equation equal to 1 and proposed
317 Eq. (15) to calculate the hydraulic gradient.

318 $$i = \frac{f}{d}.\frac{V^2}{g} \tag{15}$$

According to the equations presented in fluid mechanics, Eq. (16) is presented to calculate the friction force applied to the assumed control volume of porous media materials (Streeter 1962).

$$F_f = \gamma A h_f \tag{16}$$

The drag force is also expressed using Eq. (17) (Batchelor and Batchelor 2000).

$$F_d = C_d \gamma A \frac{V^2}{2g} \tag{17}$$

The external friction force is equal to the drag force. In other words, by equating Eqs. (16) and (17), Eq. (18) was obtained.

$$h_f = C_d \frac{V^2}{2g} \tag{18}$$

Where V is the flow velocity (m/s), g is the acceleration of gravity (m/s^2), and C_d is the drag coefficient. By performing several experiments, (Haider and Levenspiel 1989; Swamee and Ojha 1991; Ganser 1993; Chien 1994; Cheng 1997) proposed empirical equations for calculation of the drag coefficient.

To calculate the energy loss (h_f), by equating the Darcy-Wiesbach equation (Eq. 13) and the equation obtained from drag force (Eq. 18), Eq. (19) was obtained.

$$C_d = f \frac{L}{d} \tag{19}$$

Equation (19) indicates that for a given value of the friction coefficient (f), the value of the drag coefficient (C_d) and consequently, the drag force (F_d) can be calculated. In order to calculate f in terms of Reynolds number in porous media, Eq. (20) was proposed by Ahmed and Sunada using the Navier-Stokes equations in steady flow condition (Ahmed and Sunada, 1969).

$$f = \frac{1}{\mathrm{Re}} + 1, \quad \mathrm{Re} = \frac{\rho V d}{\mu} \tag{20}$$

Where ρ is water density (1000 kg/m3) and μ is water viscosity (0.001 kg/m.s). According to Eqs. (19) and (20), the drag coefficient in the free surface porous media is calculated using Eq. (21).

$$C_d = \left(\frac{1}{\mathrm{Re}} + 1\right)\frac{L}{d} \tag{21}$$

Where d is calculated using the equations proposed by Ahmed and Sunada (1969) (Eq. 7, $K = cd^2$).

Results of the present study showed that the friction coefficient (f) in one-dimensional confined porous media in the steady and unsteady flow conditions is different from Eq. (20).

3.3 Drag coefficient of steady flow in porous media

According to Darcy-Wiesbach equations (Eq. 15), the binomial equation (Eq. 3), and the equation of coefficients a and b presented by Ahmed and Sunada (Eq. 7), the friction coefficient (f) in one-dimensional confined porous media in the steady flow condition is calculated using Eq. (22).

$$f = \frac{2idg}{V^2} = \frac{2\left(\frac{\mu}{\rho g K} V + \frac{1}{g\sqrt{CK}} V^2\right) dg}{V^2} \tag{22}$$

With simplification, Eq. (24) can be written as Eq. (23).

$$f = \frac{2}{C}\left(\frac{\mu}{\rho V d} + 1\right) = \frac{2}{C}\left(\frac{1}{\mathrm{Re}} + 1\right) \tag{23}$$

In other words, in the steady flow condition in one-dimensional confined porous media, the friction coefficient (f) is 2/C times the friction coefficient (f) in the free surface porous media.

The present study considering the steady flow condition in one-dimensional confined porous media included the following steps:

1) Using experimental data, hydraulic gradient (i) (Fig. 4) in terms of flow velocity (V), the optimized coefficients a and b using the PSO algorithm (Table 2), coefficients K, C and d using Eq. (7) were calculated for small, medium and large-grained particles and summarized in Table (4).

2) The friction coefficient (f) using Eq. (15), which is the same as the observational friction coefficient, Reynolds number (Re) using Eq. (20), computational friction coefficient (f) using the presented equation in the present study (Eq. 23) was calculated for the three gradations. Figure 6 shows the changes in the friction coefficient (f) versus Reynolds number of steady flow.

3) Observational friction coefficient (calculated directly from experimental data and Eq. (15)) was compared with computational friction coefficient (calculated using Eq. (23), which was presented in the present study for steady flow condition) and mean relative error (MRE) values are shown in Table 4.

Table 4. Coefficients K, C, d and mean relative error (MRE) values obtained from observational and computational friction coefficients (f) in steady flow condition

Coefficients	Small	Medium	Large
K	9.6E-9	12.8E-9	17.1E-9
C	263.041	4331.704	8154.079
d	6.051E-6	1.717E-6	1.448E-6
MRE %	1.913	3.614	3.322

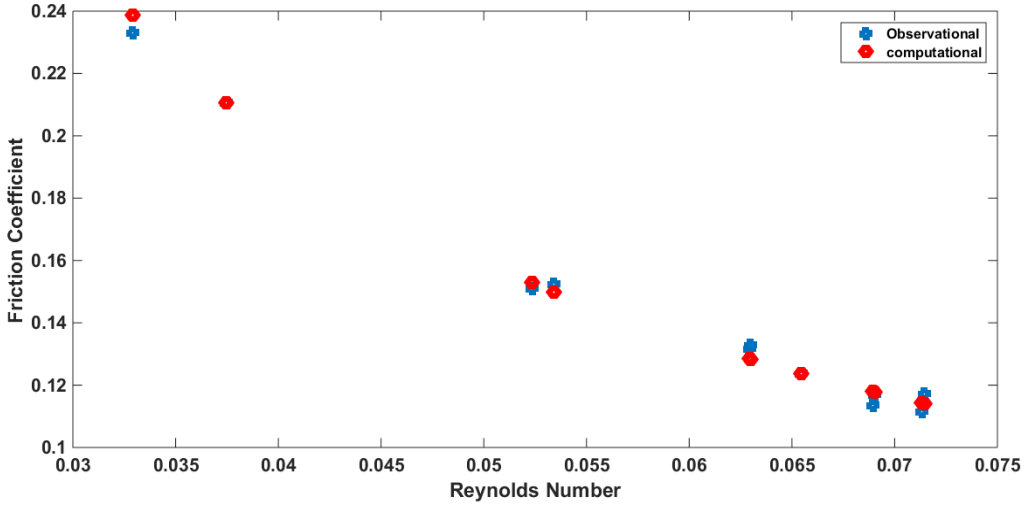

a. Small

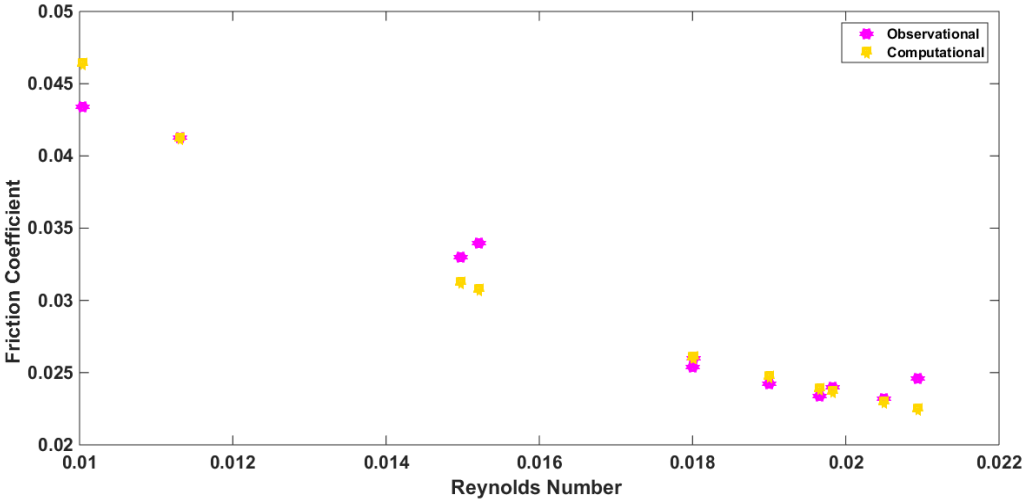

b. Medium

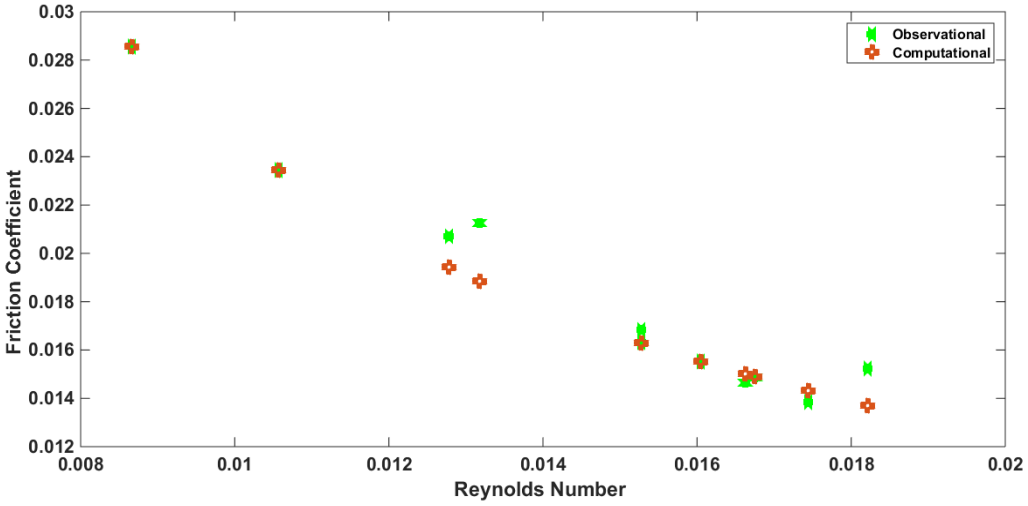

c. Large

Figure 6. Observational and computational friction coefficient versus Reynolds number in steady flow condition

385 The mean relative error (MRE) values in Table 4 and Figure 6 indicated the high accuracy
386 and efficiency of the analytical equation proposed in the present study for calculation of the
387 coefficient f and consequently, C_d and drag force (F_d) in the steady flow condition in one-
388 dimensional confined porous media.

389 **3.3 Drag coefficient of unsteady flow in porous media**

390 According to Table 3, the trinomial equation (Eq. 9) is more accurate in estimation of the
391 hydraulic gradient of unsteady flow.

392 According to the Darcy-Wiesbach equations (Eq. 15), the trinomial equation (Eq. 9) and the
393 equation presented by Ahmad and Sunada (Eq. 7) for calculation of coefficients a and b, the
394 friction coefficient (f) in one-dimensional confined porous media in unsteady flow condition
395 is calculated using Eq. (24).

396 $$f = \frac{2idg}{V^2} = \frac{2\left(\frac{\mu}{\rho g K}V + \frac{1}{g\sqrt{CK}}V^2 + c\frac{dV}{dt}\right)dg}{V^2} \quad (24)$$

397 By simplification, the coefficient f in confined porous media is obtained using Eq. (25).

398 $$f = \frac{2}{C}\left(\frac{\mu}{\rho V d}+1\right) + \frac{2dg}{V^2}.c\frac{dv}{dt} = \frac{2}{C}\left(\frac{1}{\mathrm{Re}}+1\right) + \frac{2dg}{V^2}.c\frac{dv}{dt} \quad (25)$$

399 Where C is the coefficient f obtained from the Ahmad and Sunada equation (Eq. 7) and c is
400 the coefficient of the third term of the trinomial equation (Eq. 9).

401 The calculation steps in the unsteady flow condition are the same as those for the steady flow
402 condition, with the difference that in the former, coefficients of the proposed trinomial
403 equation presented in Table 3 were used. In addition, to calculate the computational
404 coefficient f in terms of Re, the equation presented in the present study for unsteady flow (Eq.
405 25) was used.

406 The values of the coefficients K, C, d and mean relative error (MRE) values between the
407 observational and computational friction coefficients (f) for three gradation types are shown
408 in Table 5. Changes in the observational and computational f in terms of Re are also shown in
409 Figure 7.

410 **Table 5.** Coefficients K, C, d and mean relative error (MRE) values obtained from
411 observational and computational friction coefficients (f) in unsteady flow condition

Coefficients	Small	Medium	Large
K	35.7E-9	45.8E-9	27.5E-9
C	2.344	8.298	32.865
d	123E-6	74.3E-6	28.9E-6
MRE %	7.806	14.106	10.506

412

413

414

415

416

417

418

419

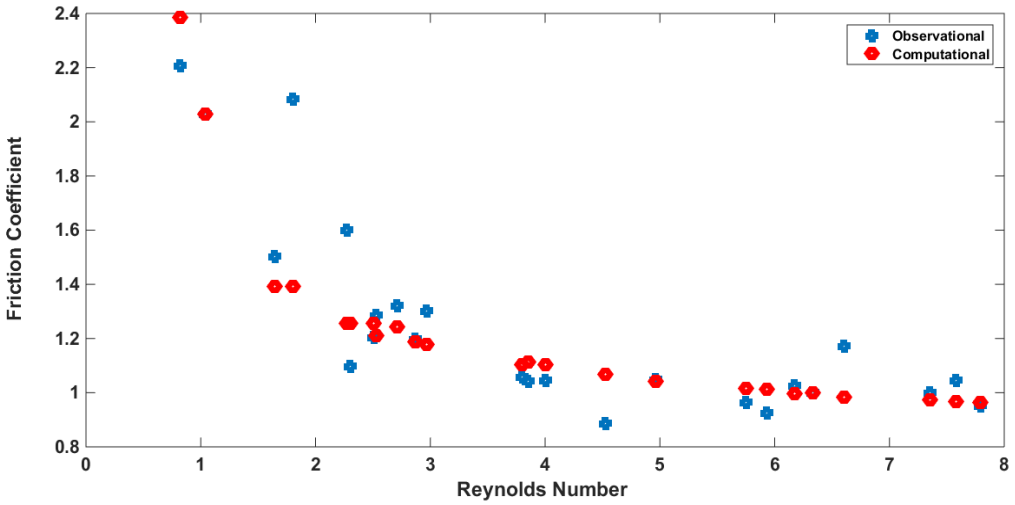

420

421 **a.** Small

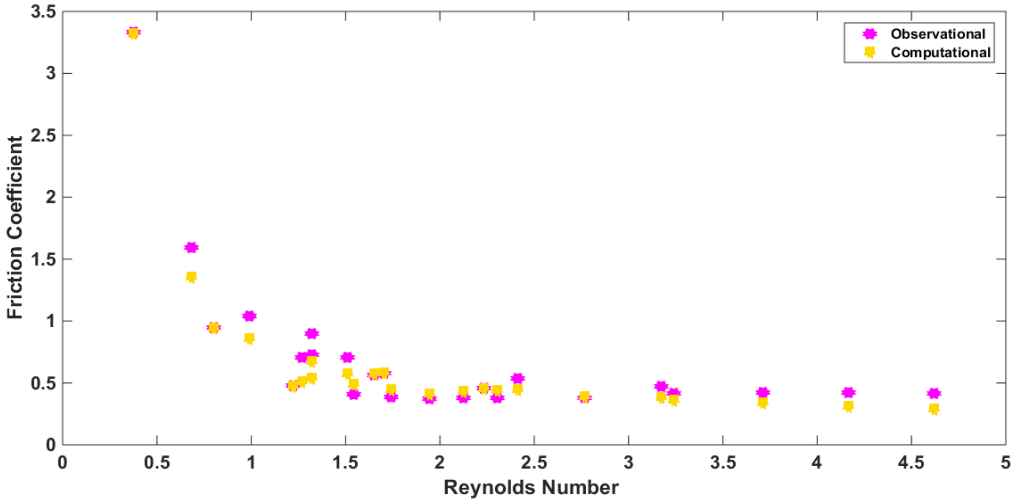

422

423 **b.** Medium

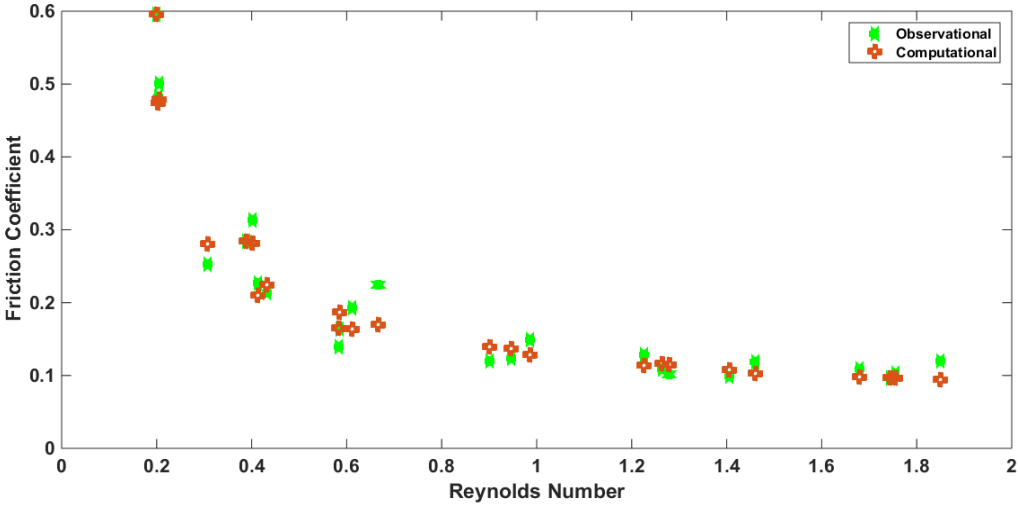

424

425 **c.** Large

426 **Figure 7.** Changes in observational and computational friction coefficients in terms of
427 Reynolds number in unsteady flow condition

The mean relative error (MRE) values (Table 5) as well as the changes in the observational and computational f values in terms of Re (Fig. 6) indicated the high accuracy and efficiency of the proposed equation in the present study to calculate f and consequently, C_d and F_d for unsteady flow in one-dimensional confined porous media.

4 Conclusions

In the present study, steady and unsteady flows in one-dimensional confined porous media were studied to calculate the changes in hydraulic gradient (i) in terms of flow velocity (V) and drag force (F_d) considering small, medium and large grained materials. The calculation of drag coefficient (C_d) is the most important step in calculations of F_d. On the other hand, according to performed studies, the only important parameter in calculation of the C_d in a porous media is the friction coefficient (f). For this reason, in the present study, to calculate the coefficient f in terms of Reynolds number (Re), the Darcy-Wiesbach equation in pipes, the equations of i in terms of V (in the steady flow condition as a binomial equation and in the unsteady flow condition as a trinomial equation), and the analytical equation by Ahmad and Sunada in calculation of the coefficients a, b and coefficient f in terms of Re in porous media, an equation for steady flow condition and another equation for unsteady flow condition in one-dimensional confined porous media were presented, which have many applications in civil engineering, mechanics, geology, and oil industry. The proposed equations for the f coefficient in terms of Re in both steady and unsteady flow conditions were evaluated using experimental data and the results showed the accuracy and efficiency of these equations in estimation of the coefficient f and consequently, C_d and F_d. In general, the results of the present study include the followings.

1) Comparison of the accuracy of the hydraulic gradient calculations in terms of flow velocity in unsteady flow conditions with the methods of a) trinomial equation, b) binomial equation

and coefficients a and b obtained from unsteady flow data by assuming an insignificant coefficient c, and C) binomial equation and coefficients a and b obtained from steady flow data showed that the methods a to c are more accurate, respectively.

2) Mean relative error (MRE) values between observational coefficients f in the steady flow condition (direct use of experimental data to calculate coefficient f) and computational f coefficients (using the proposed equation in the present study to calculate coefficient f in the steady flow condition) for small, medium and large grained materials were equal to 1.913, 3.614 and 3.322%, respectively.

3) By using the proposed equation in the present study to calculate the coefficient f in unsteady flow condition and then, comparing the computational and observational f values, the mean relative error (MRE) values of 7.806, 14.106 and 10.506% were obtained for the small, medium and large grained materials, respectively.

In other words, the results indicated that trinomial equation is more accurate in calculation of the hydraulic gradient changes with respect to the unsteady flow velocity. In addition, to calculate the coefficient f in terms of Re and consequently, the coefficient C_d in the porous media, instead of using the experimental and numerical equations obtained for a certain number of particles in the laboratory, the proposed equations in the present study for the steady and unsteady flow conditions with any number of particles and for all Reynolds numbers are suitably accurate and efficient.

Funding: The authors did not receive support from any organization for the submitted work.

Conflict of Interest: The authors have no financial or proprietary interests in any material discussed in this article.

Availability of data and material: The authors certify the data and materials contained in the manuscript.

Code availability: The relationships used are presented in the manuscript and the description of the particle swarm optimization (PSO) algorithm is also attached.

Authors' contributions: All authors have contributed to various sections of the manuscript.

Ethics approval: The authors heeded all of the Ethical Approval cases.

Consent to participate: The authors have studied the cases of the Authorship principles section and it is accepted.

Consent for publication: The authors certify the policy and the copyright of the publication.

All authors contributed to the study conception and design. Material preparation, data collection and analysis were performed by [**Hadi Norouzi**], [**Jalal Bazargan**], [**Faezeh Azhang**] and [**Rana Nasiri**]. The first draft of the manuscript was written by [**Hadi Norouzi**] and all authors commented on previous versions of the manuscript. All authors read and approved the final manuscript.

5 References

Abbas, W., Awadalla, R., Bicher, S., Abdeen, M. A., & El Shinnawy, E. S. M. (2021). Semi-analytical solution of nonlinear dynamic behaviour for fully saturated porous media. European Journal of Environmental and Civil Engineering, 25(2), 264-280.

Afshar, A., Kazemi, H., & Saadatpour, M. (2011). Particle swarm optimization for automatic calibration of large scale water quality model (CE-QUAL-W2): Application to Karkheh Reservoir, Iran. Water resources management, 25(10), 2613-2632.

Ahmed, N. and Sunada, D. K. 1969. Nonlinear flow in porous media. Journal of the Hydraulics Division, 95(6): 1847-1858.

Bari, R. and Hansen, D. (2002). Application of gradually-varied flow algorithms to simulate buried streams. Journal of Hydraulic Research. 40(6): 673-683.

Batchelor, C. K., & Batchelor, G. K. (2000). An introduction to fluid dynamics. Cambridge university press.

500 Bazargan, J., Norouzi, H. (2018). Investigation the Effect of Using Variable Values for the Parameters of the
501 Linear Muskingum Method Using the Particle Swarm Algorithm (PSO). Water Resources Management, 32(14),
502 4763-4777.

503 Bazargan, J., Shoaei, S. M., (2006). Discussion, "Application of gradually varied flow algorithms to simulate
504 buried streams." IAHR J. of Hydraulic Research, Vol 44, No 1, 138-141.

505 Bechler, A., Romary, T., Jeannée, N., & Desnoyers, Y. (2013). Geostatistical sampling optimization of
506 contaminated facilities. Stochastic environmental research and risk assessment, 27(8), 1967-1974.

507 Bird RB, & Stewart WE, Lightfoot EN. (2007). Transport phenomena. Second ed. London: John Wiley and
508 Sons.

509 Cao, K., & Ye, X. (2013). Coarse-grained parallel genetic algorithm applied to a vector based land use
510 allocation optimization problem: the case study of Tongzhou Newtown, Beijing, China. Stochastic
511 Environmental Research and Risk Assessment, 27(5), 1133-1142.

512 Chau, K. (2005). A split-step PSO algorithm in prediction of water quality pollution. In International
513 Symposium on Neural Networks (pp. 1034-1039). Springer, Berlin, Heidelberg.

514 Chau, K.W., (2007). A split-step particle swarm optimization algorithm in river stage forecasting. J. Hydrol. 34,
515 131–135.

516 Cheng, N. S. (1997). Simplified settling velocity formula for sediment particle. Journal of hydraulic
517 engineering, 123(2), 149-152.

518 Chien, S. F. (1994). Settling velocity of irregularly shaped particles. SPE Drilling & Completion, 9(04), 281-
519 289.

520 Chen, R. C., & Wu, J. L. (2000). The flow characteristics between two interactive spheres. Chemical
521 engineering science, 55(6), 1143-1158.

522 Chu, H. J., Chang, L. C. (2009). Applying particle swarm optimization to parameter estimation of the nonlinear
523 Muskingum model. Journal of Hydrologic Engineering, 14(9), 1024-1027.

524 Clerc, M., Kennedy, J., (2002). The particle swarm-explosion, stability, and convergence in a multidimensional
525 complex space. IEEE Trans. Evol. Comput. 6 (1), 58–73.

526 Di Felice, R. (1994). The voidage function for fluid-particle interaction systems. International Journal of
527 Multiphase Flow, 20(1), 153-159.

528 Di Cesare, N. Chamoret, D. and Domaszewski, M. (2015). A new hybrid PSO algorithm based on a stochastic
529 Markov chain model. Advances in Engineering Software. 90: 127-137.

530 Eberhart, R. and Kennedy, J. (1995). A new optimizer using particle swarm theory. In MHS'95. Proceedings of
531 the Sixth International Symposium on Micro Machine and Human Science (pp. 39-43). IEEE.

532 Ergun, S. (1952). Fluid Flow through Packed Columns. Chemical Engineering Progress. 48: 89–94.

533 Fand, R. M., & Thinakaran, R. (1990). The influence of the wall on flow through pipes packed with spheres.

534 Forchheimer, P. (1901). Wasserbewagung Drunch Boden, Z.Ver, Deutsh. Ing. 45: 1782-1788.

535 Ganser, G. H. (1993). A rational approach to drag prediction of spherical and nonspherical particles. Powder
536 technology, 77(2), 143-152.

537 Gudarzi, M., Bazargan, J., Shoaei, S. (2020). Longitude Profile Analysis of Water Table in Rockfill Materials
538 Using Gradually Varied Flow Theory with Consideration of Drag Force. Iranian Journal of Soil and Water
539 Research, 51(2), 403-415. doi: 10.22059/ijswr.2019.287292.668295

540 Gurarslan, G., Karahan, H., (2011). Parameter Estimation Technique for the Nonlinear Muskingum Flood
541 Routing Model. In: 6thEWRA International Symposium-Water Engineering and Management in a Changing
542 Environment, Catania, Italy.

543 Hannoura, A. A., McCorquodale, J. A., (1985). Rubble Mounds: Hydraulic Conductivity Equation, J.
544 Waterway, Port, Costal and Ocean Engineering, ASCE, 111(5), 783-799.

545 Hansen, D. Garga, V. K. and Townsend, D. R. (1995). Selection and application of a one-dimensional non-
546 Darcy flow equation for two-dimensional flow through rockfill embankments. Canadian Geotechnical
547 Journal. 32(2): 223-232.

548 Haider, A., & Levenspiel, O. (1989). Drag coefficient and terminal velocity of spherical and nonspherical
549 particles. Powder technology, 58(1), 63-70.

550 Herrera, N. M., & Felton, G. K. (1991). HYDRAULICS OF FLOW THROUGH A ROCKHLL DAM USING
551 SEDIMENT-FREE WATER. Transactions of the ASAE, 34(3), 871-0875.

552 Hill, R. J., Koch, D. L., & Ladd, A. J. (2001a). The first effects of fluid inertia on flows in ordered and random
553 arrays of spheres. Journal of Fluid Mechanics, 448, 213.

554 Hill, R. J., Koch, D. L., & Ladd, A. J. (2001b). Moderate-Reynolds-number flows in ordered and random arrays
555 of spheres. Journal of Fluid Mechanics, 448, 243.

556 Hoang, H., Hoxha, D., Belayachi, N., & Do, D. P. (2013). Modelling of two-phase flow in capillary porous
557 medium by a microscopic discrete approach. European journal of environmental and civil engineering, 17(6),
558 444-452.

559 Hsu, K. C., & Chen, K. C. (2010). Multiscale flow and transport model in three-dimensional fractal porous
560 media. Stochastic Environmental Research and Risk Assessment, 24(7), 1053-1065.

561 Hu, M. C., Shen, C. H., Hsu, S. Y., Yu, H. L., Lamorski, K., & Sławiński, C. (2019). Development of Kriging-
562 approximation simulated annealing optimization algorithm for parameters calibration of porous media flow
563 model. Stochastic Environmental Research and Risk Assessment, 33(2), 395-406.

564 Ingham, D. B., & Pop, I. (Eds.). (2005). Transport phenomena in porous media III (Vol. 3). Elsevier.

565 Jiang, X., Lu, W., Na, J., Hou, Z., Wang, Y., & Chi, B. (2018). A stochastic optimization model based on
566 adaptive feedback correction process and surrogate model uncertainty for DNAPL-contaminated groundwater
567 remediation design. Stochastic Environmental Research and Risk Assessment, 32(11), 3195-3206.

568 Karahan, H., (2012). Determining rainfall-intensity-duration-frequency relationship using Particle Swarm
569 Optimization. KSCE J. Civil Eng. 16 (4), 667–675.

570 Kumar, D.N., Reddy, M.J., (2007). Multipurpose reservoir operation using particle swarm optimization. J.
571 Water Resour. Plan. Manage. ASCE 133 (3), 192–201.

572 Kovács, G. (1980). Developments in water science: seepage hydraulics. Elsevier Scientific Publishing
573 Company.

574 Lei, T., Meng, X., & Guo, Z. (2017). Pore-scale study on reactive mixing of miscible solutions with viscous
575 fingering in porous media. Computers & Fluids, 155, 146-160.

576 Leps, T. M. (1973). Flow through rockfill, Embankment-dam engineering casagrande volume edited by
577 Hirschfeld, RC and Poulos, SJ.

578 Liang, S. C., Hong, T., & Fan, L. S. (1996). Effects of particle arrangements on the drag force of a particle in the
579 intermediate flow regime. International journal of multiphase flow, 22(2), 285-306.

580 Lu, W. Z., Fan, H. Y., Leung, A. Y. T., & Wong, J. C. K. (2002). Analysis of pollutant levels in central Hong
581 Kong applying neural network method with particle swarm optimization. Environmental monitoring and
582 assessment, 79(3), 217-230.

583 Mccorquodale, J. A., Hannoura, A. A. A., Sam Nasser, M. (1978). Hydraulic conductivity of rockfill. Journal of
584 Hydraulic Research, 16(2), 123-137.

585 Moghaddam, A., Behmanesh, J., Farsijani, A. (2016). Parameters estimation for the new four-parameter
586 nonlinear Muskingum model using the particle swarm optimization. Water resources management, 30(7), 2143-
587 2160.

588 Nagesh Kumar, D., Janga Reddy M. (2007). Multipurpose reservoir operation using particle swarm
589 optimization. J Water Resour Plan Manag 133:192–201.

590 Norouzi, H., Bazargan, J. (2020). Flood routing by linear Muskingum method using two basic floods data using
591 particle swarm optimization (PSO) algorithm. Water Supply.

592 Norouzi, H., & Bazargan, J. (2021). Effects of uncertainty in determining the parameters of the linear
593 Muskingum method using the particle swarm optimization (PSO) algorithm. Journal of Water and Climate
594 Change.

595 Rahimi, M., Schoener, Z., Zhu, X., Zhang, F., Gorski, C. A., & Logan, B. E. (2017). Removal of copper from
596 water using a thermally regenerative electrodeposition battery. Journal of hazardous materials, 322, 551-556.

597 Rong, L. W., Dong, K. J., & Yu, A. B. (2013). Lattice-Boltzmann simulation of fluid flow through packed beds
598 of uniform spheres: Effect of porosity. Chemical Engineering Science, 99, 44-58.

599 Schlichting, H., Gersten, K. (2000). Boundary layer theory, eighth ed. Springer Verlag, Berlin.

600 Sedghi-Asl, M., Rahimi, H. (2011). Adoption of Manning's equation to 1D non-Darcy flow problems. Journal of
601 Hydraulic Research, 49(6), 814-817.

602 Stephenson, D. J. (1979). Rockfill in hydraulic engineering. Elsevier scientific publishing compani. Distributors
603 for the United States and Canada.

Sidiropoulou, M. G. Moutsopoulos, K. N. Tsihrintzis, V. A. (2007). Determination of Forchheimer equation coefficients a and b. Hydrological Processes: An International Journal. 21(4): 534-554.

Sheikh, B., & Pak, A. (2015). Numerical investigation of the effects of porosity and tortuosity on soil permeability using coupled three-dimensional discrete-element method and lattice Boltzmann method. Physical Review E, 91(5), 053301.

Sheikh, B., & Qiu, T. (2018). Pore-scale simulation and statistical investigation of velocity and drag force distribution of flow through randomly-packed porous media under low and intermediate Reynolds numbers. Computers & Fluids, 171, 15-28.

Shi, Y. and Eberhart, R. (1998). A modified particle swarm optimizer. In 1998 IEEE international conference on evolutionary computation proceedings. IEEE world congress on computational intelligence (Cat. No. 98TH8360) (pp. 69-73). IEEE.

Shokri, M., Saboor, M., Bayat, H., Sadeghian, J. (2012). Experimental Investigation on Nonlinear Analysis of Unsteady Flow through Coarse Porous Media. Journal of Water and Wastewater; Ab va Fazilab (in persian), 23(4), 106-115.

Song, Z., Li, Z., Wei, M., Lai, F., & Bai, B. (2014). Sensitivity analysis of water-alternating-CO2 flooding for enhanced oil recovery in high water cut oil reservoirs. Computers & Fluids, 99, 93-103.

Streeter, V. L. (1962). Fluid mechanics, McCraw-Hill Book Company.

Swamee, P. K., & Ojha, C. S. P. (1991). Drag coefficient and fall velocity of nonspherical particles. Journal of Hydraulic Engineering, 117(5), 660-667.

Van der Hoef, M. A., Beetstra, R., & Kuipers, J. A. M. (2005). Lattice-Boltzmann simulations of low-Reynolds-number flow past mono-and bidisperse arrays of spheres: results for the permeability and drag force. Journal of fluid mechanics, 528, 233.

Ward, J. C. (1964). Turbulent flow in porous media. Journal of the hydraulics division. 90(5): 1-12.

Wen, C. Y., & Yu, Y. H. (1966). A generalized method for predicting the minimum fluidization velocity. AIChE Journal, 12(3), 610-612.

Yin, X., & Sundaresan, S. (2009). Fluid-particle drag in low-Reynolds-number polydisperse gas–solid suspensions. AIChE journal, 55(6), 1352-1368.

Zhang, Y., Ge, W., Wang, X., & Yang, C. (2011). Validation of EMMS-based drag model using lattice Boltzmann simulations on GPUs. Particuology, 9(4), 365-373.

Zhang, T., Du, Y., Huang, T., Yang, J., Lu, F., & Li, X. (2016). Reconstruction of porous media using ISOMAP-based MPS. Stochastic environmental research and risk assessment, 30(1), 395-412.

Zhu, C., Liang, S. C., & Fan, L. S. (1994). Particle wake effects on the drag force of an interactive particle. International journal of multiphase flow, 20(1), 117-129.

Zhu, X., Rahimi, M., Gorski, C. A., & Logan, B. (2016). A thermally-regenerative ammonia-based flow battery for electrical energy recovery from waste heat. ChemSusChem, 9(8), 873-879.

1. Particle Swarm Optimization Algorithm

This algorithm was first introduced by Eberhart and Kennedy in 1995 (Eberhart and Kennedy, 1995). The Particle Swarm Optimization Algorithm is a population-based search algorithm such as genetic algorithm, ant colony algorithm, bee algorithm, etc. It is a nature-inspired algorithm designed based on collective intelligence and social behavior of birds and fish (Abido, 2002). The advantages of the Particle Swarm Optimization Algorithm include simple structure and implementation, low number of controllable parameters and high convergence speed as well as high computational efficiency (Abido, 2002; Del Valle et al. 2008). The structure of this algorithm will be discussed below.

1.1 Initial population creation

This algorithm starts by generating a random number of particles. Each of these particles is a possible answer to the optimization problem. Increasing the number of particles makes the algorithm complex. Of course, this increase in the initial population reduces the number of iterations of the algorithm. There must be a compromise between these two parameters. The number of this initial population as well as the number of iterations of the algorithm depends on the type and nature of the optimization problem.

In Particle Swarm Optimization Algorithm, each particle i has a position vector and a velocity vector, which are defined as equations (1) and (2) (Clerc, 2010).

$$x_i = [x_{i1}, x_{i2}, ..., x_{in}] \tag{1}$$

$$v_i = [v_{i1}, v_{i2}, ..., v_{in}] \tag{2}$$

x_i : The current location of the i_{th} particle

v_i : The current speed of the i_{th} particle

n in the above equations is the dimension of the search space of the optimization problem.

The Particle Swarm Optimization Algorithm must consider a variable that holds the best position of each particle in its memory. This variable is considered as x^{iBest}. Where i is considered to represent the number of the particle. In the other word, x^{iBest} is cost function having the lowest value (or the profit or fitness function having the highest value). In the next step, after generating a random initial population, the variables x^{iBest} and x^{gBest} must be quantified according to equations 3 and 4 . In equation 3, x^{gBest} is the best particle among the community of particles. As x^{gBest} does not belong to any particular particle, index i has not been applied. As seen in equation 4, at this stage of the algorithm, because the particles have no motion, and are newly generated, x^{iBest} is equal to x_i. x^{iBest} is the best personal experience of the i_{th} particle (Clerc, 2010).

$$x^{gBest}(t+1)=\begin{cases} x_i(\mathrm{t}) & Cost(x_i(\mathrm{t}))<Cost(x^{gBest}) \\ x^{gBest} & Cost(x_i(\mathrm{t}))>Cost(x^{gBest}) \end{cases} \quad (3)$$

$$x^{iBest}(\mathrm{t}+1)=x_i(\mathrm{t}) \quad (4)$$

1.2 The particles movement toward the best particle

At this stage of the algorithm, a movement should be considered for the particles generated in the previous section. Equation 3 is used to change the location of each particle. In this equation, two random functions of r_1 and r_2 with uniform distribution are used to model the stochastic

nature of the algorithm. Speed update equation is in the form of equation 5. In this equation, r_1 and r_2 are scaled using c_1 and c_2. In this equation, $0<c_1, c_2<2$, that these coefficients are known as Acceleration Coefficients. It is called so because if the value of equation 5 is rewritten as the equation 6, by dividing the two sides of the equation 6 in unit of time, the value on the left of the equation represents the acceleration coefficients. The acceleration coefficients have an effect on each step of each particle in each reiteration. In the other word, the value of c_1 represents the affectivity of a particle from its best memory position and the value of c_2 represents the affectivity of the particle from the total. In equations 5 and 6, index j represents the j_{th} dimension of each particle in which j is j-0,1,….n (Eberhart and Kennedy, 1995).

$$v^i[t+1] = v^i[t] + c_1 r_{1,j}(x^{iBest}[t] - x^i[t]) + c_2 r_{2,j}(x^{gBest}[t] - x^i[t]) \quad (5)$$

$$v^i[t+1] - v^i[t] = c_1 r_{1,j}(x^{iBest}[t] - x^i[t]) + c_2 r_{2,j}(x^{gBest}[t] - x^i[t]) \quad (6)$$

In the above equation, over time, if a particle has cost function less (or benefit function higher than) the x^{gBest}, it will replace this particle and the cost value and position of the particle will be updated. The speed update equation has three components. The first component of this equation corresponds to the velocity of the particle in the previous step and is therefore called the inertia component. This component reflects the tendency of the particle group to maintain its orientation in the search space. As shown in Equation (6), the performance of the algorithm is influenced by the best position of each particle, the best individual experience of the particle (the best individual experience of the particle) as well as the position of the best neighbor particle in the neighborhood of the same particle (the best collective experience). Therefore, each particle with a special ratio will be attracted toward its best value and its best neighbor particle. Therefore, the

second component of this equation is called the cognitive component and the third component is called the social component.

1.3 Inertia coefficient

The value of velocity vector $v^i[t]$ in equation (5) can be considered as a variable. This vector is weighted by w which is called the inertia coefficient. This parameter is one of the important parameters in the Particle Swarm Optimization Algorithm that its proper tuning makes this algorithm robust (Ting et al. 2012). This parameter was first introduced by Shay and Eberhart in 1998 and added to the velocity equation (Shi and Eberhart, 1998). By incorporating this parameter into Equation (5), it is modified into Equation (6) (Di Cesare et al. 2015). To improve the convergence of the algorithm, the coefficient can be adjusted so that it decreases by passing time and approaching to the optimal response. Adjusting this parameter provides a variety of linear, nonlinear, and adaptive functions such as Constant inertia weight, Random inertia Weight, linear decreasing inertia weight, Oscillating Inertia Weight, etc. in reference (Bansal et al. 2011), the authors have discussed 15 of these functions and have investigated the performance of these functions on function 5, which is discussed in the following sections. The decreasing trend of the inertia coefficient and consequently the decrease of the inertia component of the velocity equation is due to the particle moving initially with larger steps and as approaching to the final answer to the optimization problem, decreasing the particles step makes the particles not to get far from the optimal response. This modification can be done by multiplying coefficient w into a damping constant, so that at the end of each iteration in the main circle of this algorithm, this constant is re-multiplied into w. Moreover, the value of inertia coefficient can be defined as equation (8) (Eberhart et al. 2001; Lee and Park, 2006). In this equation, ω_{min} and ω_{max},

respectively, represent the initial and final values of inertia coefficient and $Iter$ and $Iter_{Max}$ represent Current iteration number and iteration number.

$$v^i[\mathrm{t}+1] = w\,\mathrm{v}^i[t] + c_1 r_{1,j}(\mathrm{x}^{iBest}[\mathrm{t}] - \mathrm{x}^i[\mathrm{t}]) + c_2 r_{2,j}(\mathrm{x}^{gBest}[\mathrm{t}] - \mathrm{x}^i[\mathrm{t}]) \tag{7}$$

$$w = \omega_{Max} - \frac{\omega_{Max} - \omega_{Min}}{Iter_{Max}} \times Iter \tag{8}$$

Given the neighborhood concept of each particle and the social intelligence of the Particle Swarm Optimization Algorithm or the third component of equation (7), topologies are presented as follows.

1.4 Particle Swarm Evolutionary Algorithm Models

In general, the Particle Swarm Optimization Algorithm is examined by two main models. 1) Global best model (Gbest) and Local best model (Lbest). The main difference between the two models is in structure of the neighborhood model of each particle. In the first model, the neighborhood of each particle contains all members of the population and only one particle is known as the best particle, and all the particles in the group are absorbed by it. In this model, the best particle information is shared with the rest of the particles. Unlike the Gbest model, in Lbest, each particle only has access to the information related to the neighborhood of the same particle. In Gbest model, because all particles of the group is absorbed by a single particle, this model has a higher convergence rate than the Lbest model. One on the other, the probability of this model being trapped at local extreme points is higher than in the case of several defined neighborhoods (Poli et al. 2007; Mavrovouniotis et al. 2017).

For these models several topologies are presented which will be explained in the next section.

1.5 Types of network topologies or structures

1.5.1 Definition of particle topology

Particle topology is the symbolic network structure of particles that reflects how the population particles interact and share information with each other.

As mentioned in the previous sections, this algorithm can be defined as a set of particles moving in areas determined by the best successful experience of each particle and the best experience of some other particles. According to the phrase "best experience of some other particles", there are many structures in the references that three main cases will be discussed below.

1. Star

2. Ring (Circles)

3. Wheel

1.5.2 Star structure

In the star structure, all the particles in the group are adjacent to each other. Therefore, the position of the best particle of the group is shared with all the particles of the group and affects their velocity updating equation. This structure is related to the Gbest model. In this structure, the probability of being trapped at the optimal local point is increased if the best solution of the problem is not close to the best particle. The properties of this structure can be attributed to its rapid convergence as well as the greater likelihood of being trapped in optimal local locations. The star structure is shown in the figure 1.

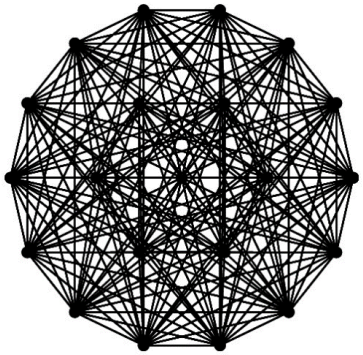

Fig. 1. Star structure

1.5.3 Ring (Circles) structure

In this structure, each particle is adjacent to its n particle. So that there are n/2 particles on each side. This structure for state n=2 is shown in Fig. (2). In this case, each particle is associated with its two adjacent particles. This structure is corresponding to the Lbest model. In this structure, each particle strives to move toward the best particle in its defined neighborhood. In this structure more areas of the search space are examined, but the convergence rate of this structure is low (Kacprzyk, 2009).

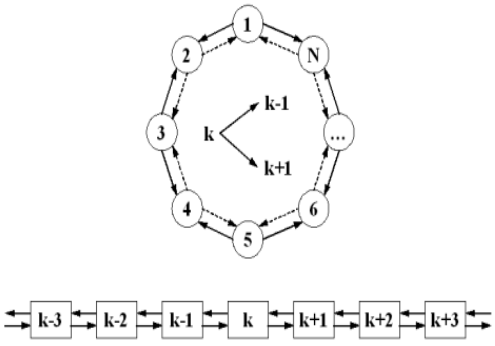

Fig. 2. Ring structure in n=2

1.5.4 Wheel structure

In the wheel structure, one particle is considered as the Focal particle (Hub). In this structure, the middle particle is attached to all the particles in the group, but the other particles are only attached to this particle and are insulated from each other. The focal particle moves to the best particle. If this focal particle movement improves its performance, it also affects other particles. This structure is shown in Fig. 3.

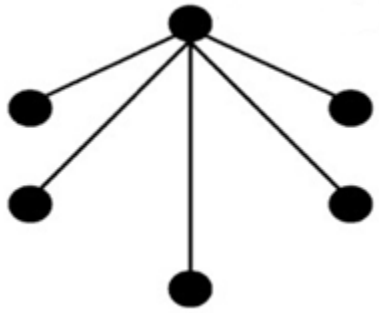

Fig. 3. Wheel structure

1.6 Improved convergence of Particle Swarm Optimization Algorithm

Morris Clarke and James Kennedy have proposed a method for selecting coefficients in equation (7) to improve the convergence of Particle Swarm Optimization Algorithms. In this method, equation (7) is modified in form of equation (9) (Clerc and Kennedy, 2002).

$$v^i[\mathrm{t}+1] = \chi(\mathrm{v}^i[t] + c_1 r_{1,j}(\mathrm{x}^{iBest}[\mathrm{t}] - \mathrm{x}^i[\mathrm{t}]) + c_2 r_{2,j}(\mathrm{x}^{gBest}[\mathrm{t}] - \mathrm{x}^i[\mathrm{t}])) \tag{9}$$

In the recent equation, χ is Constriction coefficient which is defined as equation (10).

$$\chi = \frac{2}{\left|2 - \varphi - \sqrt{\varphi^2 - 4\varphi}\right|} \tag{10}$$

In the recent equation, coefficient φ is defined as equation 11 (Chan et al. 2007).

$$\varphi = c_1 + c_2 \qquad \varphi > 4 \tag{11}$$

1.7 Limiting velocity

After obtaining the particle velocity vector of the group, it is necessary to check whether the velocities obtained are within the specified permissible range. This allowed range is usually expressed as a coefficient of the width of the search space. This range is shown in Equations (12) and (13).

$$v_{\max} = \alpha(x_{\max} - x_{\min}) \tag{12}$$

$$v_{\min} = -\alpha(x_{\max} - x_{\min}) \tag{13}$$

In both recent equations, x_{min} and x_{max} represent the variables range in optimization problem. In addition, Alpha coefficient has a value between zeros to one, so that the velocity threshold value does not exceed the width of the research space.

After determining the particle velocity vector and determining the particle velocity threshold, these ranges are applied as relation (14):

$$v^{i,j}(t+1) = \begin{cases} v_{\min} & v^{i,j}(t+1) \le v^{j}{}_{\min} \\ v^{i,j}(t+1) & v^{j}{}_{\min} < v^{i,j}(t+1) < v^{j}{}_{\max} \\ v_{\max} & v^{i,j}(t+1) \ge v^{i,j}{}_{\max} \end{cases} \tag{14}$$

At this point, new values of group particle velocity are set and the necessary constraints are applied. Now the new position of the particles must be determined. This new position is determined by Equation (15).

$$x(t+1) = x(t) + v(t+1) \tag{15}$$

Displacement of the particle based on the velocity update equation and the displacement equation has been shown in Fig. (4). After the displacement of the particle following the mentioned steps, the above steps are repeated until the termination conditions of the algorithm are satisfied and the best particle position among all the group members is delivered as the optimal response.

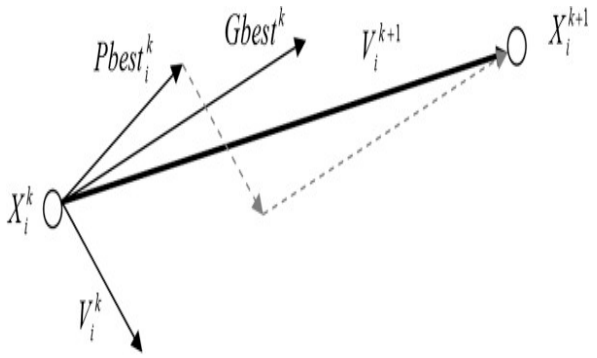

Fig. 4. Displacement of the i_{th} particle in Particle Swarm Optimization Algorithm

References

Abido, M. A. (2002). Optimal design of power-system stabilizers using particle swarm optimization. IEEE transactions on energy conversion, 17(3), 406-413.

Bansal, J. C., Singh, P. K., Saraswat, M., Verma, A., Jadon, S. S., & Abraham, A. (2011, October). Inertia weight strategies in particle swarm optimization. In Nature and Biologically Inspired Computing (NaBIC), 2011 Third World Congress on (pp. 633-640). IEEE.

Clerc, M. (2010). Particle swarm optimization (Vol. 93). John Wiley & Sons.

Clerc, M., & Kennedy, J. (2002). The particle swarm-explosion, stability, and convergence in a multidimensional complex space. IEEE transactions on Evolutionary Computation, 6(1), 58-73.

Chan, F. T. S., & Tiwari, M. K (2007). Swarm Intelligence: focus on ant and particle swarm optimization. I-Tech Education and Publishing. Cited on, 146.

Del Valle, Y., Venayagamoorthy, G. K., Mohagheghi, S., Hernandez, J. C., & Harley, R. G. (2008). Particle swarm optimization: basic concepts, variants and applications in power systems. IEEE Transactions on evolutionary computation, 12(2), 171-195.

Di Cesare, N., Chamoret, D., & Domaszewski, M. (2015). A new hybrid PSO algorithm based on a stochastic Markov chain model. Advances in Engineering Software, 90, 127-137.

Eberhart, R., & Kennedy, J. (1995). A new optimizer using particle swarm theory. In Micro Machine and Human Science, 1995. MHS'95., Proceedings of the Sixth International Symposium on (pp. 39-43). IEEE.

Eberhart, R. C., Shi, Y., & Kennedy, J. (2001). Swarm Intelligence (The Morgan Kaufmann Series in Evolutionary Computation).

Kacprzyk, J. (2009). Studies in Computational Intelligence, Volume 198.

Lee, K. Y., & Park, J. B. (2006, October). Application of particle swarm optimization to economic dispatch problem: advantages and disadvantages. In Power Systems Conference and Exposition, 2006. PSCE'06. 2006 IEEE PES (pp. 188-192). IEEE.

Mavrovouniotis, M., Li, C., & Yang, S. (2017). A survey of swarm intelligence for dynamic optimization: algorithms and applications. Swarm and Evolutionary Computation, 33, 1-17.

Poli, R., Kennedy, J., & Blackwell, T. (2007). Particle swarm optimization. Swarm intelligence, 1(1), 33-57.

Shi, Y., & Eberhart, R. (1998, May). A modified particle swarm optimizer. In Evolutionary Computation Proceedings, 1998. IEEE World Congress on Computational Intelligence., The 1998 IEEE International Conference on (pp. 69-73). IEEE.

Ting, T. O., Shi, Y., Cheng, S., & Lee, S. (2012, June). Exponential inertia weight for particle swarm optimization. In International Conference in Swarm Intelligence (pp. 83-90). Springer, Berlin, Heidelberg.

Figures

a

b

c

Figure 1

Schematic view of the experimental setup, a) the installed tank on the roof, b) the tank and cylinder installed in the laboratory, and c) steel cylinder

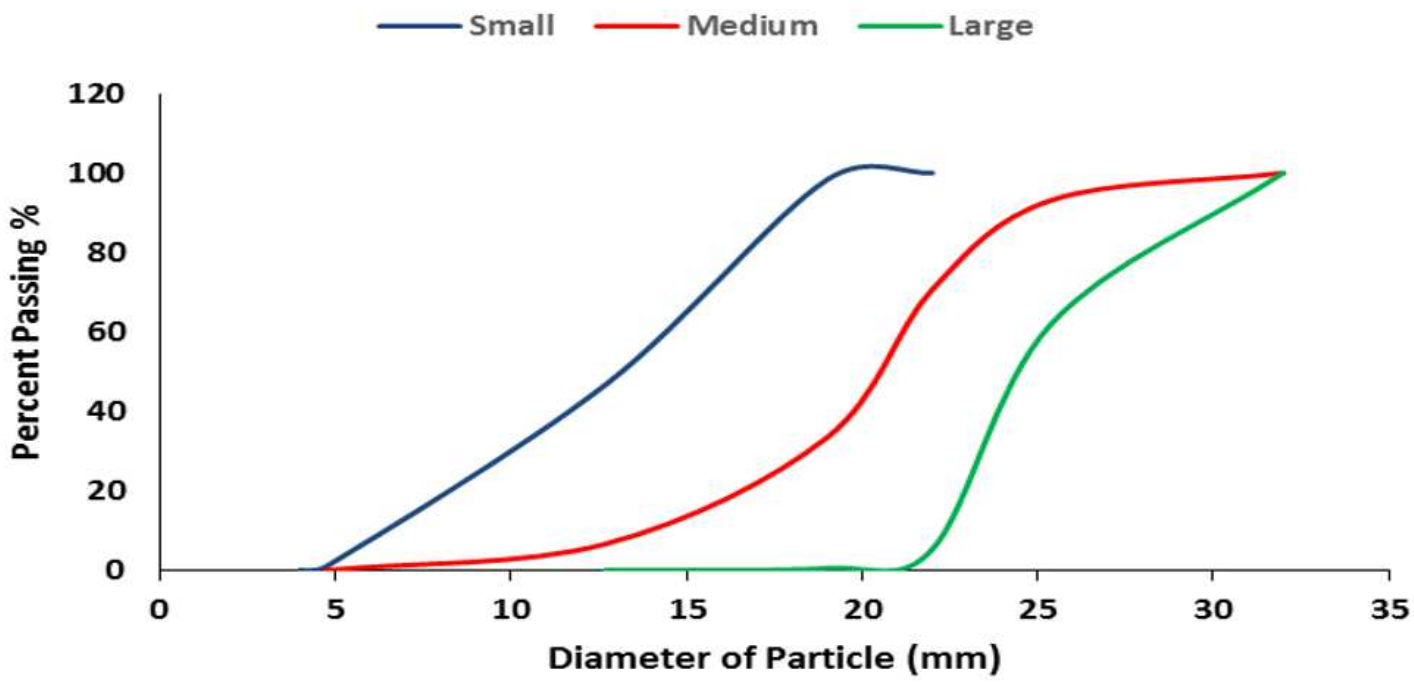

Figure 2

Gradation curve of different materials

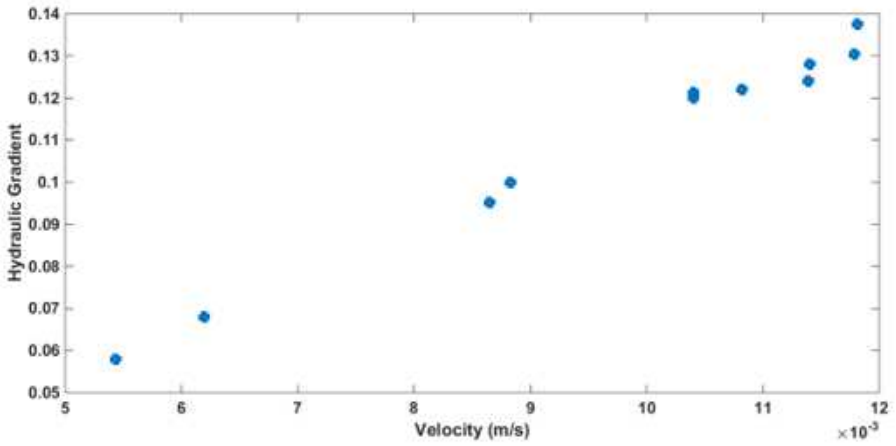

a. Small

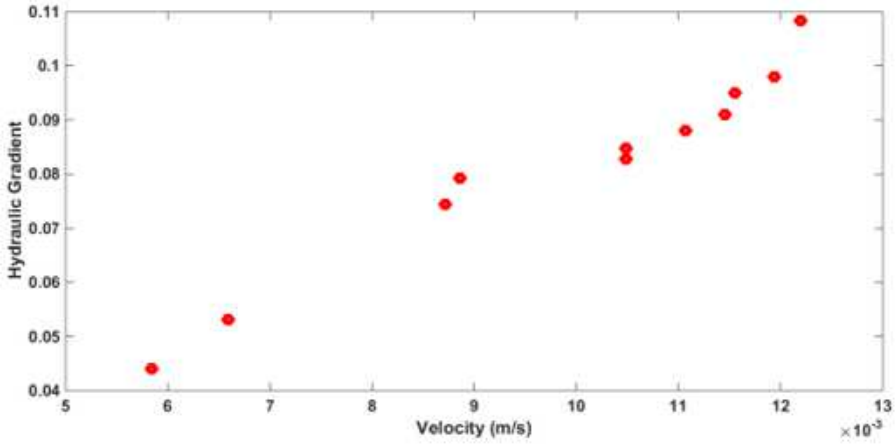

b. Medium

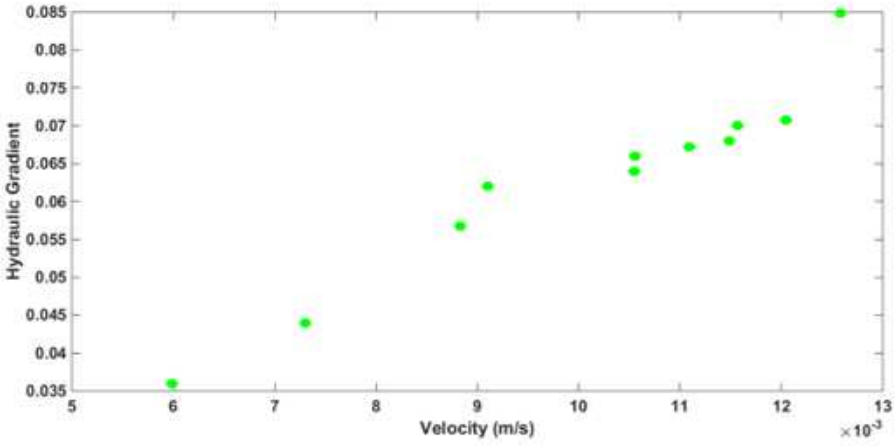

c. Large

Figure 3

Changes in hydraulic gradient versus steady flow velocity recorded in the laboratory

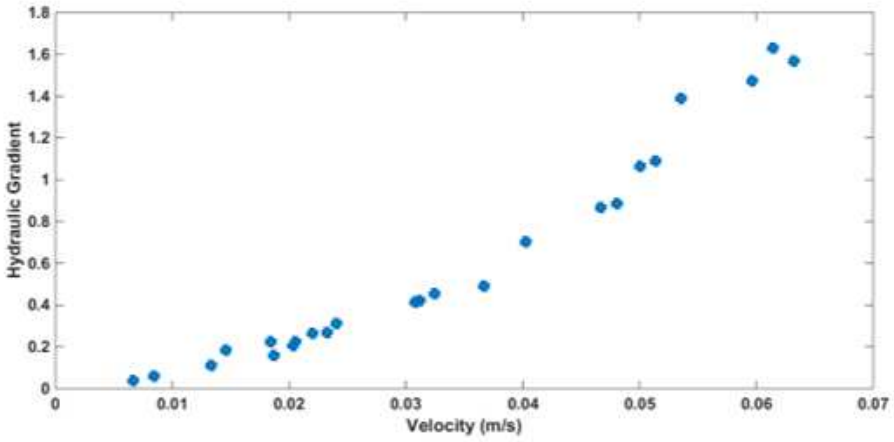

a. Small

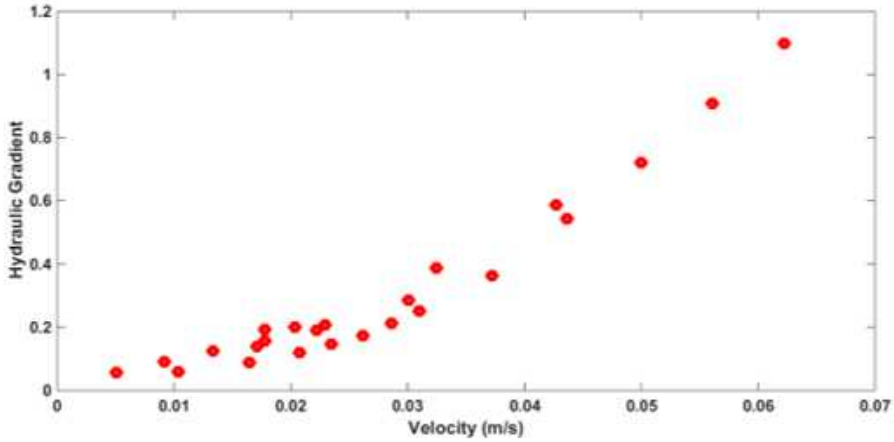

b. Medium

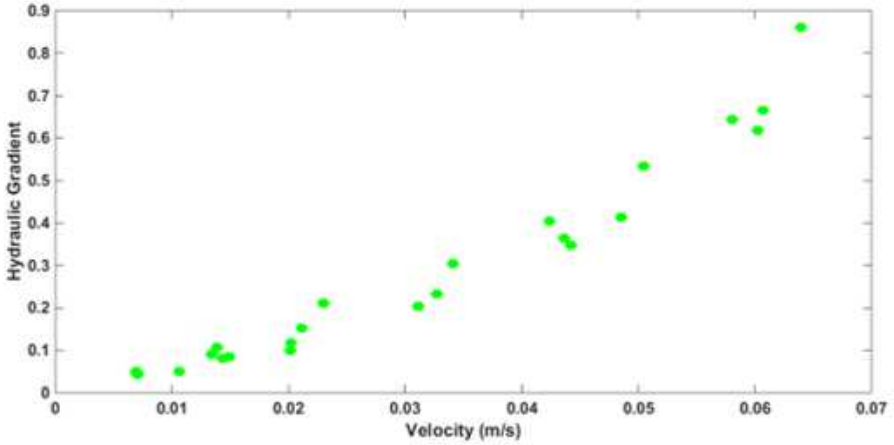

c. Large

Figure 4

Changes in hydraulic gradient versus unsteady flow velocity recorded in the laboratory

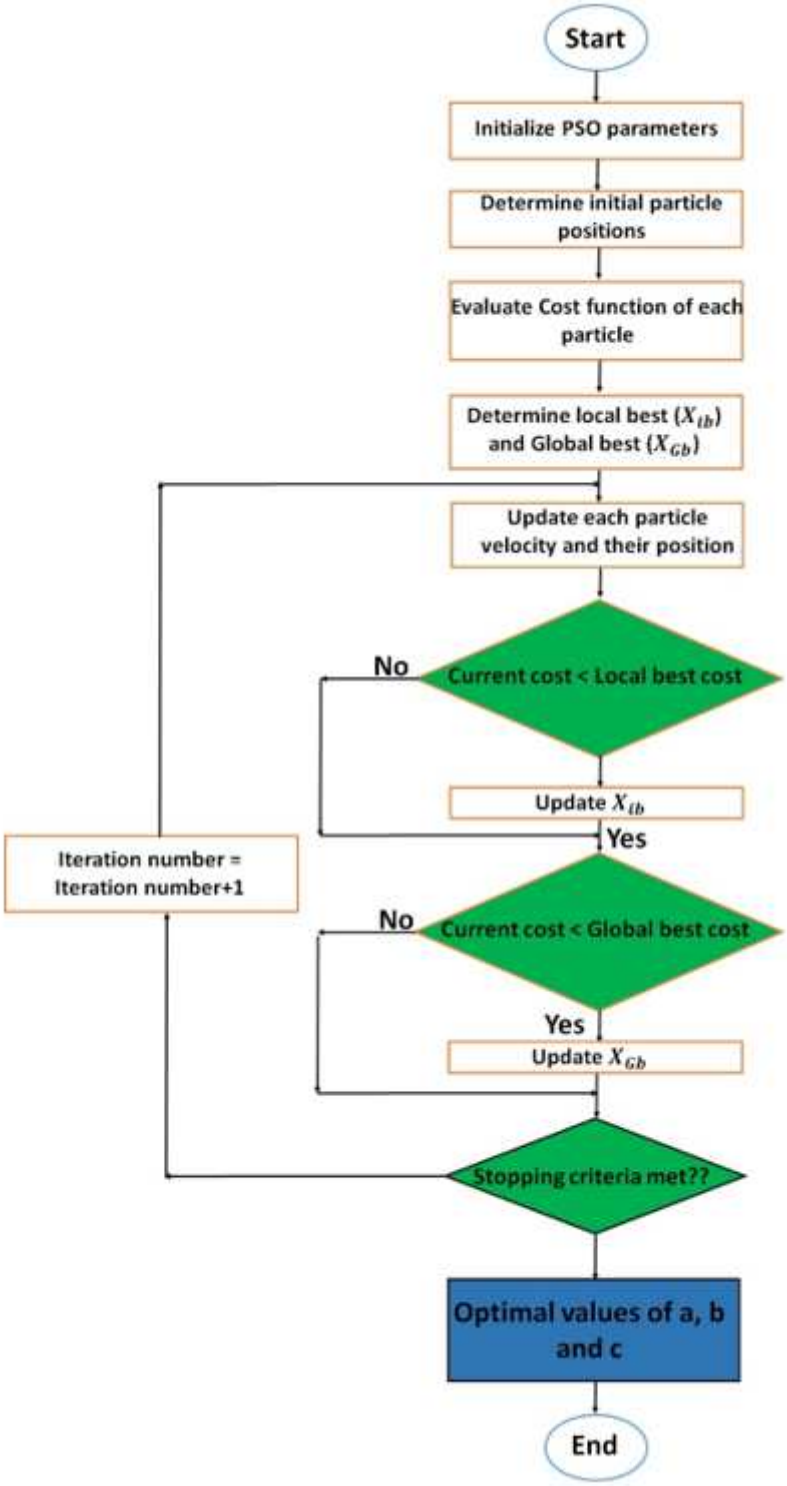

Figure 5

Particle Swarm Optimization (PSO) algorithm

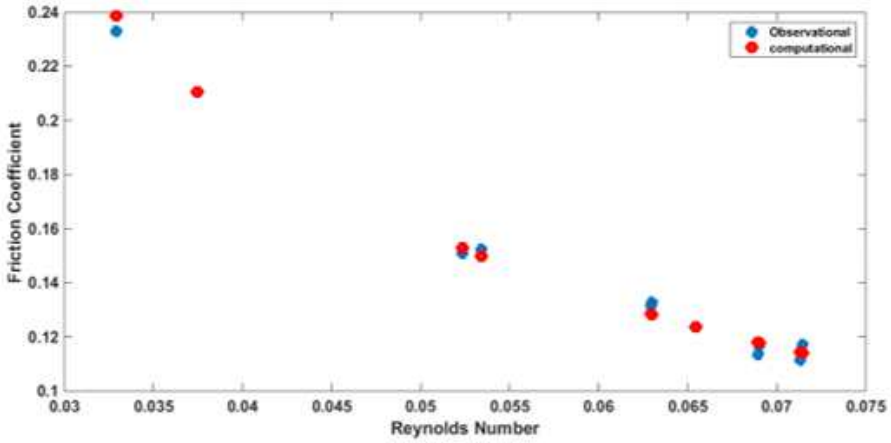

a. Small

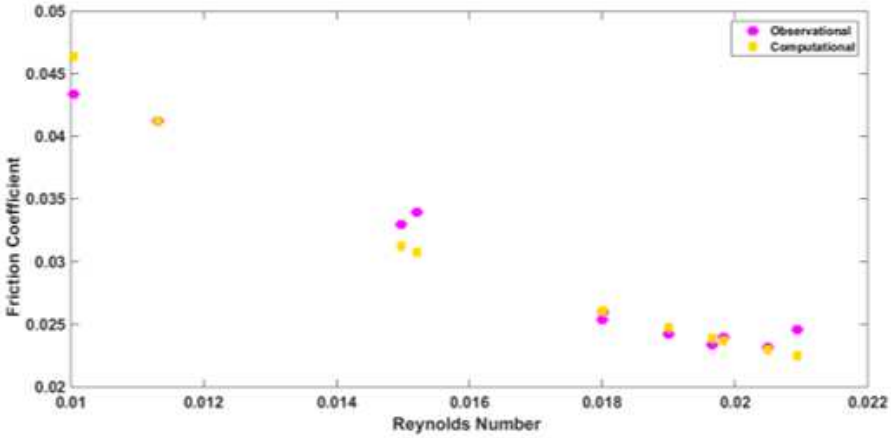

b. Medium

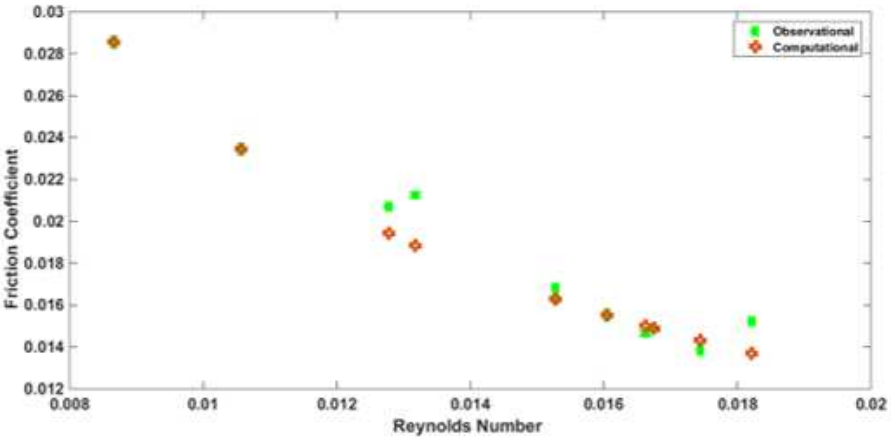

c. Large

Figure 6

Observational and computational friction coefficient versus Reynolds number in steady flow condition

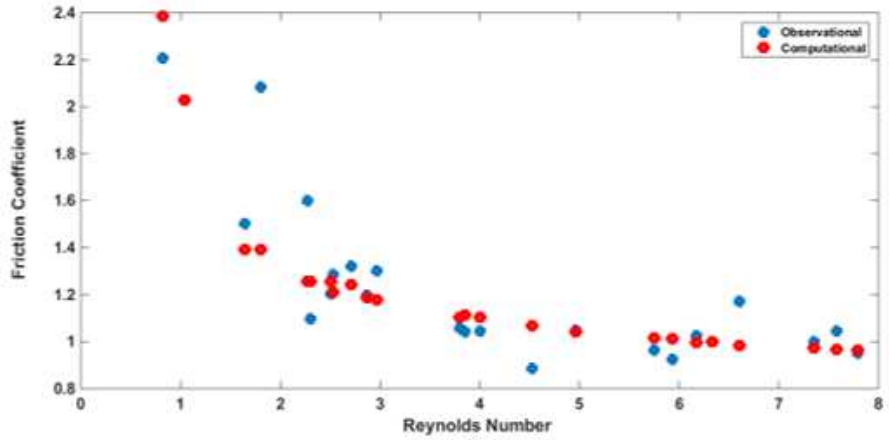

a. Small

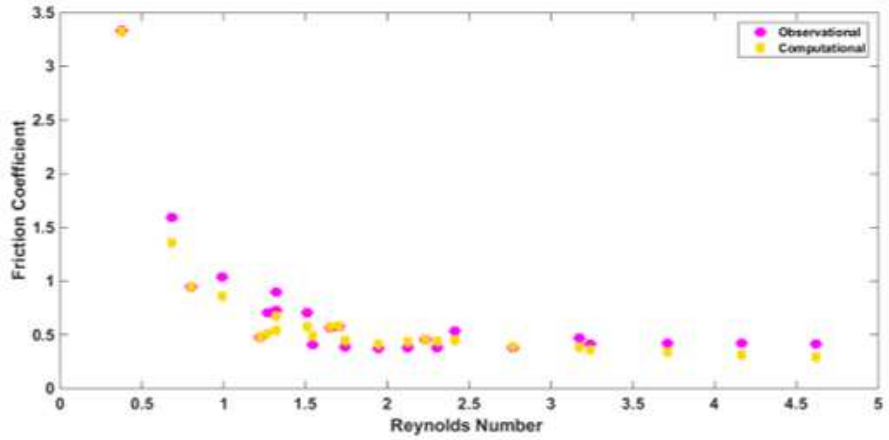

b. Medium

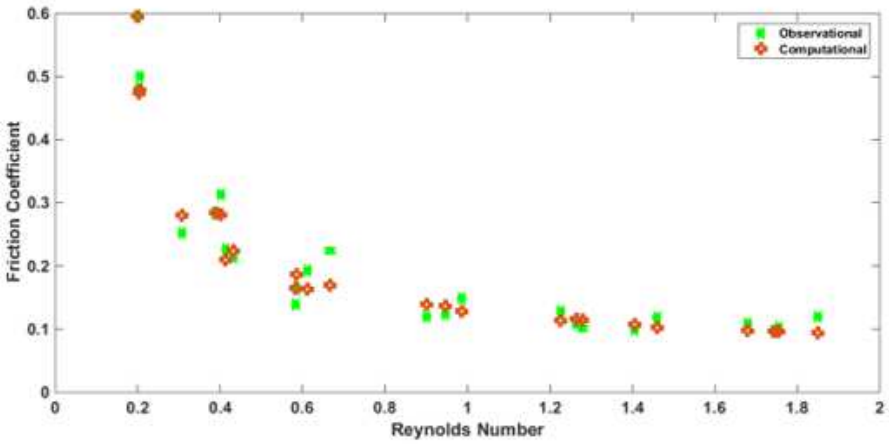

c. Large

Figure 7

Changes in observational and computational friction coefficients in terms of Reynolds number in unsteady flow condition